CEBAF Program Advisory Committee Six (PAC6) Proposal Cover Sheet

This proposal must be received by close of business on April 5, 1993 at:

CEBAF
User Liaison Office
12000 Jefferson Avenue
Newport News, VA 23606

Proposal Title

Inclusive η Photoproduction in Nuclei

Contact Person

Name: Michael F. Vineyard
Institution: University of Richmond
Address: Department of Physics
Address: University of Richmond
City, State ZIP/Country: Richmond, VA 23173
Phone: (804) 289-8257 **FAX:** (804) 289-8482
E-Mail → BITnet: VINEYARD@URVAX **Internet:** VINEYARD@URVAX.URICH.EDU

If this proposal is based on a previously submitted proposal or letter-of-intent, give the number, title and date:

CEBAF Use Only

Receipt Date: 4/2/93 Log Number Assigned: PR 93-008

By: gf

Inclusive η Photoproduction in Nuclei

M. F. Vineyard (Spokesperson),[1] S. Ahmad,[2] B. E. Bonner,[2] S. Dytman,[3]
H. Funsten,[4] G. P. Gilfoyle,[1] C. E. Hyde-Wright,[5] B. J. Lieb,[6] R. W. Major,[1]
B. A. Mecking,[7] R. A. Miskimen,[8] G. S. Mutchler,[2] B. G. Ritchie,[9]
P. D. Rubin,[4] J. B. Seaborn,[1] H. Stroeher,[10] and A. Yegneswaran[7]

[1]University of Richmond
[2]Rice University
[3]University of Pittsburgh
[4]College of William and Mary
[5]University of Washington
[6]George Mason University
[7]CEBAF
[8]University of Massachusetts
[9]Arizona State University
[10]University of Giessen

Abstract

We propose to measure inclusive η photoproduction in nuclei (^{2}H, ^{3}He, ^{4}He, ^{12}C, ^{58}Ni, ^{208}Pb) over the photon energy range k = 0.8-1.5 GeV. The experiment will be performed with the CEBAF Large Acceptance Spectrometer (CLAS) and the bremsstrahlung photon tagging system in Hall B. The neutral mesons will be detected via the 2γ decay mode. These measurements will provide important information on the ηN interaction and nuclear-medium modifications of N* resonances.

1. Scientific Motivation

Over the last fifteen years, significant progress has been made in understanding the pion-nucleus interaction. However, very little information exists on the interaction of the next simplest meson, the eta, with nucleons, and almost nothing is known about its interaction with nuclei. The study of the η meson shares many of the motivations of the study of the pion. Just as the pion studies have provided extensive information on the $\Delta(1232)$ and its dynamics within the nuclear medium, the investigation of the η, with its isospin selectivity, should enable us to obtain a similar understanding of the $S_{11}(1535)$ and other isospin-1/2 N* resonances. In addition, due to the lack of η beams, the production of η mesons in nuclei will provide important information on the η-nucleon and η-nucleus interactions. Reactions induced with photons are particularly suitable for these studies because photons probe the entire nuclear volume.

The current understanding of the photoproduction of η mesons is based on a rather sparse data set. Most of this data is 20 years old [1], with the exception of two more recent measurements [2,3]. The data base will soon improve, however, as extensive photoproduction measurements [4] are planned at CEBAF. These measurements will be complemented by an electroproduction experiment [5] at CEBAF to study the $S_{11}(1535)$ and $P_{11}(1710)$ resonances which are the only nucleon resonances of mass less than 2 GeV with significant η decay branches. The results of these upcoming experiments should improve our knowledge of the elementary (γ,η) process significantly.

Attempts to describe the elementary amplitudes involved in the (γ,η) reaction have focussed on several different theoretical approaches. In one approach [2,6,7], the process is described in terms of known nucleon resonances and a phenomenological background. This model contains a large number of parameters which must be determined from fits to the available data.

An effective Lagrangian method has been used by Benmerrouche and Mukhopadhyay [8]. This approach has fewer parameters to be fitted to the data. They found that the reaction was dominated by the excitation of the $S_{11}(1535)$ resonance, and they extracted a value for the helicity amplitude $A_{1/2}$ which is compatible with quark-model estimates [9-12].

Bennhold and Tanabe [13] developed an isobar model for η photoproduction on nucleons by using the $\pi N \rightarrow \pi N$, $\pi N \rightarrow \pi\pi N$, and $\pi N \rightarrow \eta N$ reactions to determine the hadronic vertices, and the pion photoproduction reactions to parameterize the electromagnetic vertices. The η

photoproduction amplitude was then used to estimate the cross sections for coherent and incoherent η production on several nuclei. The model was later extended [14] to include Born terms in the elementary production amplitude. The results of these studies indicate that coherent and incoherent nuclear cross sections are on the order of several 10 nb.

In a series of papers by Liu and collaborators [15-17], an isobar model was used to study the η interaction with hadrons. This model predicted an attractive ηN interaction and indicated the possible existence of bound ηN states in nuclei with $A \geq 12$. In the most recent of these papers [17], the authors conclude that the widths of these bound states may be rather large.

Very recently, Carrasco [18] performed a theoretical study of inclusive η photoproduction in nuclei. In this work the many-body calculations of the N*(1535) width of Ref. [17] for the case of bound η states was extended to the problem of η propagation through nuclei. The inclusive η photoproduction cross sections through the excitation of the N*(1535) resonance were calculated with a model which incorporates nuclear-medium modifications of the N*(1535) decay width, Fermi sea effects, and final-state interactions. The photon energy dependence of the cross sections per nucleon on ^{16}O and ^{208}Pb are shown in Fig. 1. The dot-dashed curves shown in the figure are the results of calculations with the impulse approximation. The dashed curves are the nuclear cross sections which were calculated taking into account changes in the N* width, Fermi motion, and Pauli blocking effects. The solid curves are the results of the full calculations which also include final-state interactions. As can be seen in the figure, η mesons can be produced below the production threshold on the free nucleon (k = 709 MeV) due to the Fermi motion of the nucleons in the nucleus.

The target mass dependence of the cross sections at k = 800 MeV calculated with this model is shown in Fig. 2. The cross section is found to increase as A^{α} with $\alpha \cong 0.6$. This behavior is similar to that found for π^0 photoproduction on nuclei in the Δ-resonance region where the A-dependence was described by $\sigma_A \propto A^{0.66}$ [19], and indicates that particles produced in the interior of the nucleus have a small chance of escaping. In fact, Carrasco reported [18] that, according to his calculations, about 40% of the η mesons are absorbed before leaving the ^{16}O nucleus, and about 65% are absorbed in the case of ^{208}Pb. The number of η mesons which are rescattered before leaving the nucleus is calculated to be about 9% for ^{16}O and 13% for ^{208}Pb.

Shown in Fig. 3 are the differential cross sections ($d^2\sigma/d\Omega dP_{\eta}$) calculated by Carrasco [18] for ^{16}O and ^{208}Pb at k = 800 MeV and $\theta = 25^{\circ}$ before (dashed curves) and after (solid curves)

final-state interactions. The inclusion of the final-state interactions has a greater effect on the magnitude of the cross sections than it does on the shape of the distributions.

The calculations discussed above show that both final-state interactions and nuclear-medium modifications are important in inclusive η photoproduction in nuclei at energies around the $S_{11}(1535)$ resonance. Additional theoretical work must be performed on the role of other resonances and background terms in order to have a complete description of the reaction. However, it is clear that measurements of the inclusive (γ,η) cross section will provide important information on the ηN interaction and the nuclear-medium modifications of the S_{11} response. In fact, since the cross sections for coherent and incoherent photoproduction of η mesons are predicted [13,14] to be quite small (several 10 nb), inclusive measurements may be the only feasible way to study the dynamics of the N*(1535) in the nuclear medium. These measurements are necessary if further theoretical progress is to be made in this area.

At present there is very little data available on inclusive η production in nuclei. Most of these experiments have been performed with pion beams [20-24]. Some of the results of this work are illustrated in Figs. 4-6 taken from Ref. [20]. Shown in Fig. 4 is an inclusive (π^+,η) spectrum taken on ^{12}C at a beam momentum of 680 MeV/c. Energy-integrated (π^+,η) inclusive cross sections plotted as a function of target mass are shown in Fig. 5 for three values of beam momentum. The dotted curves shown in the figure are the results of Glauber model calculations [25]. The ηN total cross section, which is the only unknown input in this calculation, was adjusted to obtain the best fit to the data. A good description of the mass dependence at all three beam momenta is obtained with $\sigma(\eta N) = 15$ mb. This should be compared to the πN total cross section of 34 mb at this energy. The ηN total cross sections are displayed as a function of pion beam momentum in Fig. 6. The solid curve shown in the figure is the prediction of the additive quark model [26]. The results of this calculation are in rather good agreement with the data. The πN total cross section, shown as the dashed curve for comparison, is clearly larger than the ηN cross sections over a wide momentum range. The η momentum range of the proposed experiment is indicated above Fig. 6.

It is important to point out a disadvantage in using pion beams to make these measurements. Pion absorption and scattering in the initial state introduces an uncertainty in the extracted ηN cross section which is not present in the photoproduction reaction. The effect of the pion initial-state interactions is illustrated in Fig. 5. We have added the solid line to the figure to show the A dependence of the cross section without initial-state or final-state interactions. This cross section

scales linearly with A. The difference between this line and the dotted curve for $\sigma_{\eta N} = 0$ mb is due to the π interaction in the initial state. In the case of the photoproduction reaction, any deviation from the linear dependence will be due to η absorption in the final state.

The inclusive (p,η) reaction on nuclei has been investigated in recent experimental [27] and theoretical [28] papers. The A dependence of the differential cross section measured [27] at a proton bombarding energy of 1 GeV is shown in Fig. 7. The solid and dashed curves are the predictions of a folding model [28] with and without η absorption, respectively. The result of the folding model calculation without η absorption (dashed curve) has a greater slope than the data. This suggests significant η absorption in the nucleus. However, the calculation with absorption (solid curve) underpredicts the data, and the fact that it increases more slowly with increasing A than the data indicates that η absorption is overestimated by the model. It has been suggested [27] that this is due to the fact that η absorption is evaluated with the assumption that all η mesons are produced at the center of the nucleus. The ηN absorption cross section used in the folding model calculations was estimated by detailed balance from the $\pi^- p \rightarrow \eta n$ reaction assuming that both reactions proceeds through the N*(1535) resonance. The resulting ηN total cross section (solid curve) is shown as a function of the kinetic energy of the η meson in the nucleon rest frame in Fig. 8. The dashed curve is the result of a coupled-channel analysis of Bhalerao and Liu [15]. The two results are in good agreement.

Recently, experiments were performed at the Mainz microtron (MAMI) to measure the photoproduction of η mesons from ^{1}H, ^{2}H, ^{12}C, ^{40}Ca, ^{93}Zr, and ^{nat}Pb in the photon energy range 600-790 MeV [29]. In these experiments the neutral mesons were detected with the Two Arm Photon Spectrometer (TAPS), which consists of BaF_2 arrays. The data are still being analyzed, and only very preliminary results are available. Shown in Fig. 9 are raw mass spectra taken on several of the targets. The hatched areas in the the figure are the π^0 and η peaks which stand well above the background.

This brief discussion of inclusive η production, though incomplete, shows that both the η energy spectrum and target mass dependence of the inclusive cross section are strongly influenced by final-state interactions, and are therefore sensitive to the features of the ηN interaction. Further progress in understanding the ηN interaction is impossible without much more extensive and precise data on inclusive η production in nuclei. The (γ,η) reaction is particularly well suited for these studies due to the absence of initial-state interactions.

We propose to measure differential cross sections for the inclusive (γ,η) reaction on ^{2}H, ^{3}He, ^{4}He, ^{12}C, ^{58}Ni, and ^{208}Pb over the photon energy range k = 0.8-1.5 GeV. The η momentum distributions and the target mass dependence of the inclusive cross section will provide information on the η-nucleon interaction. Comparisons with the data on η production from the proton [4] will yield information on the nuclear-medium modifications of the I = 1/2 N* resonances.

2. Experimental Procedure

The measurements will be performed with the CEBAF Large Acceptance Spectrometer (CLAS) in Hall B. The data on the ^{2}H target can be taken concurrently with experiment PR-89-045 [30]. The measurements on the ^{3}He, ^{4}He, and ^{12}C targets can be performed concurrently with experiment PR-91-014 [31]. Additional beam time is requested for the ^{58}Ni and ^{208}Pb target. The main features of the experiment will described in the following sections.

2.1 Beam

The reactions will be induced with tagged photons produced with the Hall B bremsstrahlung tagging system. Using an incident electron energy of 1.6 GeV, the tagged photons will have an energy range of 0.8 to 1.5 GeV. This energy range will span from the $S_{11}(1535)$ resonance to above the $P_{11}(1710)$ resonance. For the counting rate estimates, the tagged photon rate has been assumed to be 10^{7} photons/s.

2.2 Kinematics

The momentum as a function of laboratory angle for η mesons produced by photons with energies between 0.75 and 1.55 GeV is shown in Fig. 10. The dashed curves correspond to constant center-of-mass angles. It can be seen from this figure that the magic photon energy which produces recoilless η's is between 0.9 and 0.95 GeV. This is the energy range which one might expect to be most favorable for the production of bound states of the η meson in nuclei.

2.3 Neutral Meson Analysis

The neutral mesons will be detected with the CLAS via the two-photon decay. A typical event

is shown in Fig. 11. The energy E_γ, polar angle θ_γ, and azimuthal angle ϕ_γ will be measured for each photon. From this one gets the opening angle ψ between the two photons and the asymmetry parameter X, defined as

$$X = \frac{|E_{\gamma 1} - E_{\gamma 2}|}{E_{\gamma 1} + E_{\gamma 2}}.$$

The η mesons will be identified from the $\gamma\gamma$ invariant mass

$$M_{\gamma\gamma} = 2\sqrt{E_{\gamma 1} E_{\gamma 2}}\,\sin\left(\frac{\psi}{2}\right)$$

while the kinetic energy E_η and the polar production angle θ_η of the η are given by the expressions:

$$E_\eta = M_\eta \sqrt{\frac{2}{(1-\cos\psi)(1-X^2)}},$$

$$\cos\theta_\eta = \frac{E_{\gamma 1}\cos\theta_{\gamma 1} + E_{\gamma 2}\cos\theta_{\gamma 2}}{\sqrt{E_{\gamma 1}^2 + E_{\gamma 2}^2 + 2\,E_{\gamma 1}E_{\gamma 2}\cos\psi}}.$$

2.4 Acceptance

Since the 2γ decay mode will be used to detect the η mesons, the only detector components of the CLAS involved in the measurements are the shower calorimeters. Monte Carlo calculations were performed to determine the CLAS acceptance for these events. In the calculations discussed here we have assumed that the shower counter coverage will be from 8° to 45° in six sectors, with two additional calorimeter modules extending the coverage from 45° to 75° in two opposite sectors. We will consider the advantages of additional shower counter coverage in a later section.

Shown in Fig. 12 is the η momentum versus laboratory angle for events accepted by CLAS from a uniform distribution. The detection efficiency as a function of η production angle at P_η = 1.0 GeV/c and as a function of η momentum at θ_η = 0° are shown in Figs. 13 and 14, respectively. The detection efficiency peaks at about 30% at θ_η = 0° and P_η = 1.0 GeV/c, and decreases as the production angle increases or the η momentum decreases until it vanishes at about θ_η = 70° or P_η = 0.2 GeV/c.

The detection efficiency as a function of photon beam energy for photoproduction on a free proton is shown in Fig. 15. The efficiency increases from about 4% at threshold (k = 0.709 GeV) to almost 10% at k = 1.5 GeV.

2.5 Momentum Resolution

We have investigated the η momentum resolution expected in this experiment. This was done with Monte Carlo calculations which take into account the expected energy and angular resolutions of the calorimeters. The momentum resolution for 1-GeV η mesons is found to be approximately 6% (σ_P/P). A cut on the asymmetry parameter $X < 0.3$ improves the resolution to about 4% at the expense of 47% of the events.

2.6 Particle Identification

Monte Carlo calculations were also performed to investigate the particle identification which can be achieved with the CLAS. A simulated mass spectrum calculated for two coincident photons from photoproduction on a free proton at an incident energy of 1.2 GeV is shown in Fig. 16. The π^0 and η peaks are clearly discernible above the background which is shown as the dashed histogram in the figure. The main contribution to the background is from the detection of two coincident photons from different π^0s produced in the $\gamma N \rightarrow \pi^0\pi^0 N$ reaction. Other contributions to the background are from the detection of two coincident photons from different π^0s from the $3\pi^0$ decay of the η (≈32%), and from coincidences between the γ and one of the photons from the π^0 produced in the $\omega \rightarrow \pi^0\gamma$ decay (≈9%). The ω decay produces the background at large mass. The background has been suppressed in the mass spectrum displayed in Fig. 16 by excluding events in which more than two photons were detected in coincidence. The different processes contributing to the mass spectrum were weighted according to the cross sections [1] and branching ratios [32].

Two simulated mass distributions with different cuts to suppress the background are compared at incident photon energies of 0.8, 1.0, 1.2, and 1.4 GeV in Figs. 17, 18, 19, and 20, respectively. The upper panel of each figure shows a mass spectrum generated with a simple static cut on the opening angle between the two detected photons. The distribution in the lower panel of each figure was produced with the additional condition that only two photons are accepted. It can be seen from the figures that the two cuts together are quite effective at reducing the background at

all four energies. However, discriminating against events with more than two photons in coincidence may bias the data by excluding processes such as $\gamma N \rightarrow \eta\pi^0 N$. We will be able to check this by analyzing both distributions. Also, it should be pointed out that a dynamical opening angle cut can be applied to the data in the off-line analysis which should help to further suppress the background. The contributions to the background at large mass are not present in the spectra at incident photon energies of 0.8 and 1.0 GeV since the ω threshold is at 1.11 GeV.

2.5 Count Rate and Beam Time Estimates

The η mesons produced with monochromatic photons of energy k will be detected at a rate given by:

$$R(k) = \frac{N_A}{A} \cdot \sigma(k) \cdot N_\gamma(k) \cdot (\rho t) \cdot \varepsilon(k) \cdot BR$$

where N_A is Avogadro's number (6.022×10^{23}), A is the mass number of the nucleus, $\sigma(k)$ is the η photoproduction cross section, N_γ is the number of incident photons per second, (ρt) is the target thickness, $\varepsilon(k)$ is the detection efficiency, and BR is the branching ratio for the 2γ decay of the η (0.39).

In estimating the count rates, we have assumed a total tagged photon flux of 10^7 photons/s with an energy distribution which decreases as 1/k. Using energy bins of approximately 100 MeV results in seven energy bins going from 0.8 to 1.5 GeV for the 1.6-GeV incident electron energy. With these assumptions we arrive at about 1.9×10^6 photons/s in the 0.8-0.9-GeV bin and 1.1×10^6 photons/s in the 1.4-1.5-GeV bin.

The elementary η photoproduction cross section decreases from approximately 15 μb at 0.8 GeV to 1.2 μb at 1.5 GeV [1], and we have assumed that the total cross section scales as $A^{0.8}$. The results of our simulations shown in Fig. 15 indicate that the detection efficiency increases from about 4% at 0.8 GeV to 9% at 1.5 GeV. Also, we have assumed a target thickness of 1 gm/cm^2 for each of the targets.

Listed in Table 1 are the rates for the 0.8-0.9-GeV and 1.4-1.5-GeV energy bins for each of the targets calculated with the above assumptions. The counting rates decrease by a factor of about 10 as the photon energy is increased from 0.8 GeV to 1.5 GeV. At the calculated rates for the deuterium target, we would detect more than 4.1×10^5 η's at 0.8-0.9 GeV and 4.3×10^4 η's at

1.4-1.5 GeV in the 500 hours previously approved for running on this target [30]. In the 150 hours previously approved for each of the ^{3}He, ^{4}He, and ^{12}C targets [31], we will obtain a maximum of 120,000 (γ,η) counts at 0.8-0.9 GeV on ^{3}He and a minimum of 9200 at 1.4-1.5 GeV on ^{12}C. We request an additional 150 hours on each of the ^{58}Ni and ^{208}Pb targets in which we will acquire approximately 65,000 (γ,η) events in the low-energy bin on ^{58}Ni and about 5200 counts in the high-energy bin on ^{208}Pb.

2.6 Triggering

Since the η mesons will be detected via the 2γ decay mode, a neutral trigger will be needed for this experiment. The minimum opening angle between the two photons from the decay of η mesons in this experiment is 45°. Therefore, the two photons from an η decay will never hit the same calorimeter module, and neutral hits in two different modules can be used as the trigger in this experiment. It is worth pointing out here that this trigger will serve to suppress much of the background from π^0 events since the decay photons from these neutral mesons have much smaller opening angles.

The two other experiments [30,31] with which this one might run concurrently both request a single charged particle trigger. We estimate that the inclusion of this neutral trigger will increase the trigger rate by less than 10% and should have little effect on the other experiments.

2.7 Potential Future Development: Extended Shower Counter Coverage

We have investigated the effect that extended shower counter coverage would have on these measurements. The results are illustrated in Fig. 21 where the detection and background-suppression efficiencies, calculated for a photon beam energy of 1.2 GeV, are displayed as a function of the number of sectors extended from 45° to 75°. The detection efficiency (solid curve) increases from about 4% to 20% as the number of sectors extended to 75° increases from 0 to 6, while the background-suppression efficiency (dashed curve) increases from 47% to 73%.

3. Intranuclear Monte Carlo Calculations

We have performed intranuclear Monte Carlo calculations to predict the sensitivity of the differential cross sections to the ηN interactions. In these calculations, the η is created in a

quasifree production process, and the subsequent interaction of the η with the nuclear system is treated by a Monte Carlo calculation which follows the η through the nucleus. The momentum distribution of the bound nucleons is described by a density-dependent Fermi gas with a density distribution taken from electron scattering. The total η photoproduction cross section is taken from a parametrization of experimental data, and is assumed to be the same for production on the proton and neutron. The total scattering ($\eta N \rightarrow \eta N$) cross section is assumed to be 15 mb. The total absorption cross section is taken from a calculation by Bennhold and Tanabe [13].

The main features of the results of these calculations for inclusive η photoproduction are illustrated in Fig. 22 which shows η momentum distributions produced on ^{208}Pb by 1.2-GeV photons at 30 to 40° in the laboratory under various physical effects. Without final-state interactions the momentum distribution (dotted histogram) is dominated by the quasifree peak. Scattering of the outgoing η mesons (dot-dashed histogram) reduces the height of the quasielastic peak considerably and increases the yield at lower momentum. Turning on the η absorption (solid histogram) further reduces the quasifree peak and damps the scattering yield at low momentum.

The A dependence of the total cross section for inclusive η photoproduction at an incident photon energy of 1.2 GeV predicted by this model is shown in Fig. 23. The cross section scales as $A^{0.8}$. This scaling was found to be essentially independent of the incident photon energy over the range of interest in this experiment. The A dependence predicted by these calculations has a greater slope than the results of Carrasco's calculations at k = 0.8 GeV where the cross section was found to scale as $A^{0.6}$ [18]. The results reported by Carrasco are somewhat surprising when compared to the π^0 photoproduction measurements [19] where it was found that the cross section scales as $A^{0.66}$ which indicates surface production. This comparison suggests that the absorption is stronger for η mesons than for pions. However, earlier measurements of the ηN cross section with pion beams [20-24] indicate that it may be as much as a factor of two smaller than the πN cross section (see Fig. 6). Therefore, it appears that the η absorption may be overestimated in Carrasco's model.

Shown in Fig. 24 is the momentum distribution expected after 150 hours of running time on ^{12}C at k = 1.4 GeV and θ_η = 20-30°. The solid histogram shows the events generated with an intranuclear Monte Carlo calculation and the dashed histogram represents the events accepted and reconstructed by the CLAS.

The expected sensitivity of the proposed measurements to the ηN cross section is illustrated in Fig. 25. Shown in this figure is the A dependence of the ratio of the nuclear cross section per

nucleon to the deuteron cross section per nucleon calculated at k = 1.2 GeV and $0^\circ < \theta_\eta < 40^\circ$. Analyzing the data in this way will remove any dependence on the elementary production amplitudes. Also, many of the systematic errors associated with the cross section measurements will cancel. For the points shown in the figure, we have assumed that the remaining systematic uncertainty is ± 3% and the statistical uncertainties have been calculated from the count rate estimates. In the calculations shown in this figure, we have assumed that the scattering cross section σ_{scat} and the absorption cross section σ_{abs} are constant and that $\sigma_{abs}/\sigma_{scat} = 2$. Calculations were then performed for different values of $\sigma_{\eta N} = \sigma_{abs} + \sigma_{scat}$. The data points were calculated with $\sigma_{\eta N} = 45$ mb and the solid, dashed, and dot-dashed curves show the results for $\sigma_{\eta N} = 0$, 42, and 48 mb, respectively. It can be seen from the figure that we should be able to determine $\sigma_{\eta N}$ to about ± 3 mb.

4. Relation to Other Experiments

4.1 Experiments at CEBAF

This proposal can be thought of as an extension of two other experiments planned at CEBAF to study the photoproduction [4] and electroproduction [5] of η mesons from the proton. Indeed, the results of these experiments will be important in the analysis of our data. As pointed out earlier, a comparison of our results with those obtained on the proton will allow us to extract information on the ηN interaction and nuclear-medium modifications of the N* resonances.

We have indicated several times in the discussion of the experimental technique that the measurements proposed here are compatible with the kaon photoproduction experiments on deuterium [30] and ^{3}He, ^{4}He, and ^{12}C [31]. The only component of the experimental design which will be affected by this experiment is the trigger, as discussed above.

4.2 Experiment at MAMI

The quasifree photoproduction of η mesons from ^{2}H, ^{12}C, ^{40}Ca, ^{93}Zr, and ^{nat}Pb has recently been measured at MAMI over the photon energy range from 600 to 790 MeV [29]. The experiment proposed here will complement these measurements at MAMI and extend them to much higher energies.

5. Theoretical Support

A couple of theorists have already expressed interest in this experiment. Prof. C. Bennhold at George Washington University has done extensive work on the photoproduction of η mesons off nucleons and the coherent and incoherent production on nuclei and is interested in extending this work to the inclusive process.

Prof. J. B. Seaborn at the University of Richmond, with a background in pion photoproduction, has already assisted in the development of this proposal and will continue to work closely with the experimental group. He is currently on sabbatical leave at Mainz and has begun work on η photoproduction.

6. Future Directions

A natural extension of this proposal would be to perform similar measurements for the η' mesons to extract information on the η'-nucleon interaction. In the chiral limit of QCD, the η and η' mesons are predicted to have very different properties. One might therefore expect the behavior of these two mesons to be distinct. It has been suggested [33] that a comparison of the interactions of the ηN and η'N systems may provide a test of QCD and our understanding of these mesons. We have not investigated the feasibility of this experiment in detail, but will begin soon to do so.

References

[1] See compilation by H. Genzel, P. Joos, and W. Pfeil, *Photoproduction of Elementary Particles, Landolt-Bornstein*, New Series I/8 (Springer, New York, 1973), p. 278; compilation by R. Baldini *et al.*, *Total Cross Sections for Reactions of High Energy Particles*, New Series I/12b (Springer, New York, 1988), p. 361.

[2] S. Homma *et al.*, J. Phys. Soc. Japn. **57**, 828 (1988).

[3] S. A. Dytman *et al.*, Bull. Am. Phys. Soc. **35**, 1679 (1990).

[4] B. G. Ritchie *et al.*, CEBAF Experiment Proposal PR-91-008 (unpublished).

[5] S. A. Dytman *et al.*, CEBAF Experiment Proposal PR-89-039 (unpublished).

[6] F. Tabakin, S. A. Dytman, and A. S. Rosenthal, *Excited Baryons 1988,* (World Scientific, Singapore, 1989) p. 168.

[7] H. R. Hicks *et al.*, Phys. Rev. **D7**, 2614 (1973).

[8] M. Benmerrouche and Nimai C. Mukhopadhyay, Phys. Rev. Lett. **67**, 1070 (1991).

[9] R. P. Feynman, M. Kislinger, and F. Ravndal, Phys. Rev. **D3**, 2706 (1971).

[10] R. Koniuk and N. Isgur, Phys. Rev. **D21**, 1868 (1980).

[11] F. E. Close and Z. Li, Phys. Rev. **D42**, 2194 (1990).

[12] M. Warns *et al.*, Phys. Rev. **D42**, 2215 (1990).

[13] C. Bennhold and H. Tanabe, Nucl. Phys. **A530**, 625 (1991); Phys. Lett. **243B**, 13 (1990).

[14] L. Tiator, S. S. Kamalov, and C. Bennhold, presented at the National Conference on Physics of Few-Body and Quark-Hadronic Systems, Kharkov, Ukraine, June, 1992.

[15] R. S. Bhalerao and L. C. Liu, Phys. Rev. Lett. **54**, 865 (1985).

[16] Q. Haider and L. C. Liu, Phys. Lett. **172B**, 257 (1986).

[17] H. C. Chiang, E. Oset, and L. C. Liu, Phys. Rev. **C44**, 738 (1991).

[18] R. C. Carrasco, Mainz preprint MKPH-T-92-16 (1992).

[19] J. Arends *et al.*, Nucl. Phys. **A454**, 579 (1986).

[20] J. C. Peng, in *Production and Decay of Light Mesons*, edited by P. Fleury (World Scientific, Singapore, 1988), p. 102;

[21] O. Guisan *et al.*, Nucl. Phys. **B32**, 681 (1971).

[22] V. V. Barmin *et al.*, Sov. J. Nucl. Phys. **28**, 780 (1979).

[23] V. D. Apokin *et al.*, Sov. J. Nucl. Phys. **35**, 219 (1982).

[24] V. V. Arkhipov *et al.*, Sov. J. Nucl. Phys. **39**, 76 (1984).

[25] K.S. Kolbig and B. Margolis, Nucl. Phys. **B6**, 85 (1968).

[26] L.O. Abrahamian *et al.*, Phys. Lett. **44B**, 301 (1973).

[27] E. Chiavassa *et al.*, Z. Phys. **A342**, 107 (1992).

[28] W. Cassing *et al.*, Z. Phys. **A340**, 51 (1991).

[29] H. Stroeher, private communication.

[30] B. A. Mecking *et al.*, CEBAF Experiment Proposal PR-89-045 (unpublished).

[31] C. E. Hyde-Wright *et al.*, CEBAF Experimental Proposal PR-91-014 (unpublished).

[32] Particle Data Group, Phys. Rev. **D45**, 1 (1992).

[33] N. Isgur, private communication.

Table 1. Count rate estimates.

Target	R (0.8-0.9 GeV) [s^{-1}]	R (1.4-1.5 GeV) [s^{-1}]
^{2}H	0.23	0.024
^{3}He	0.22	0.022
^{4}He	0.20	0.021
^{12}C	0.16	0.017
^{58}Ni	0.12	0.012
^{208}Pb	0.092	0.0096

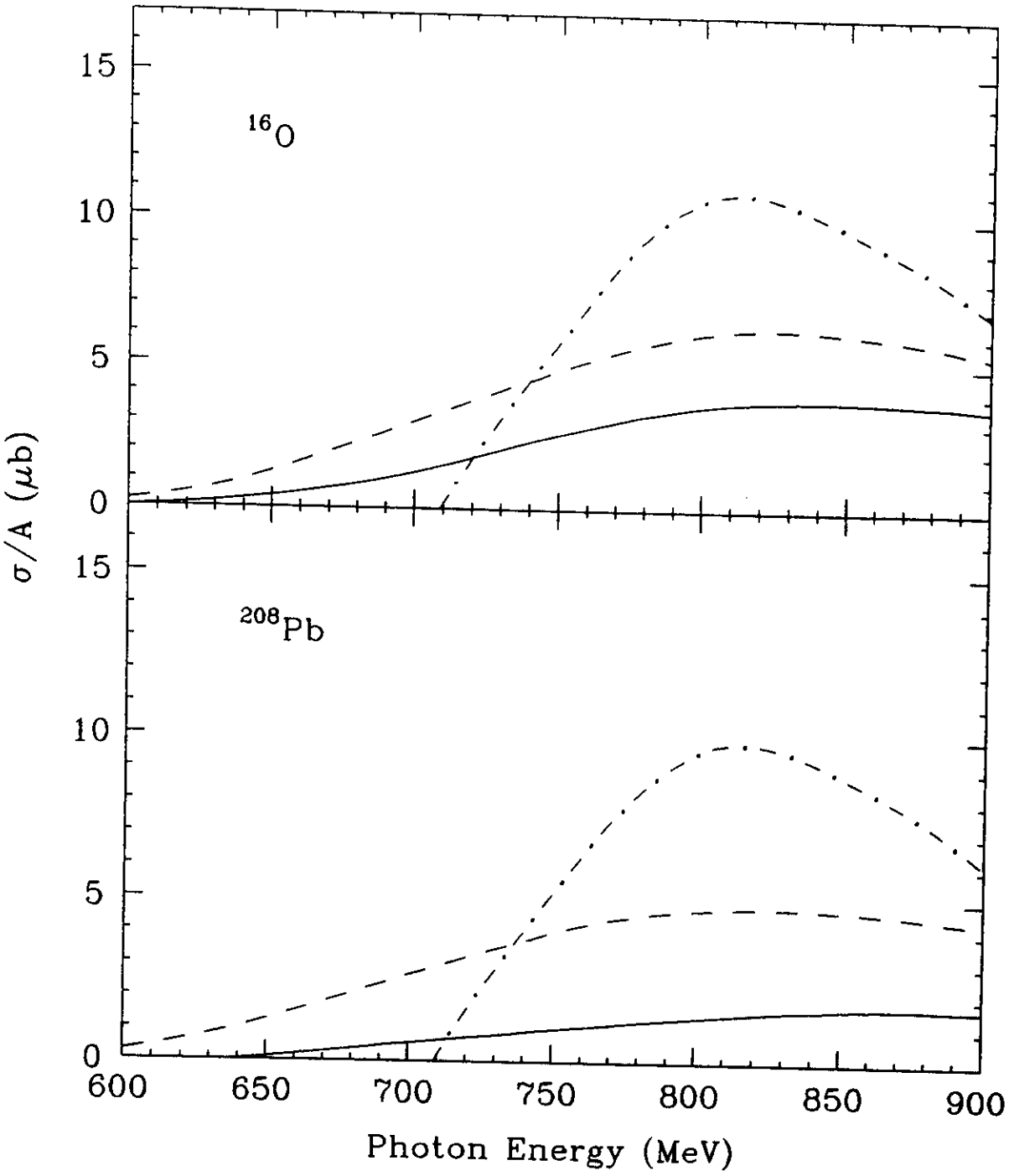

Fig. 1. Inclusive η photoproduction cross section per nucleon on ^{16}O and ^{208}Pb as a function of incident photon energy. The dot-dashed curves are the impulse approximation results. The dashed curves are the results of calculations which include Fermi sea effects and nuclear-medium modifications of the S_{11} width. The solid curves are the results of the complete calculations which also include final-state interactions. Figure reproduced from Ref. [18].

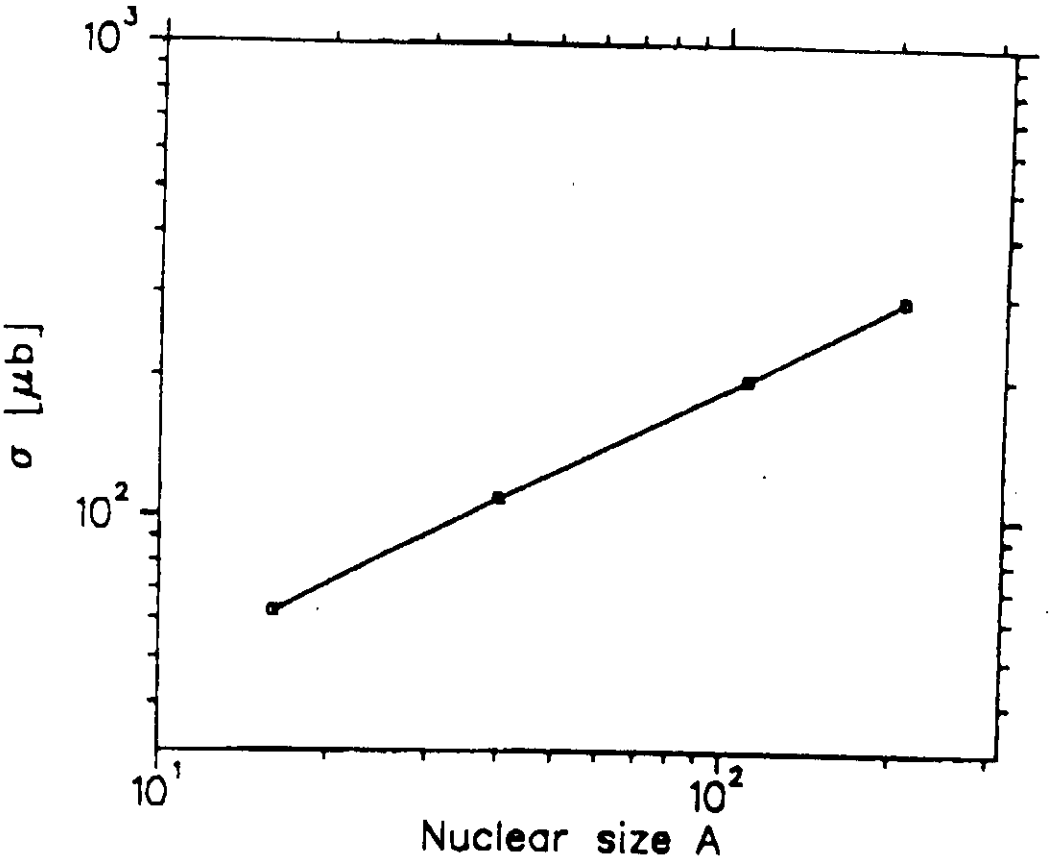

Fig. 2. Dependence of the total cross section for inclusive η photoproduction at k = 800 MeV on the nuclear mass number A. Figure taken from Ref. [18].

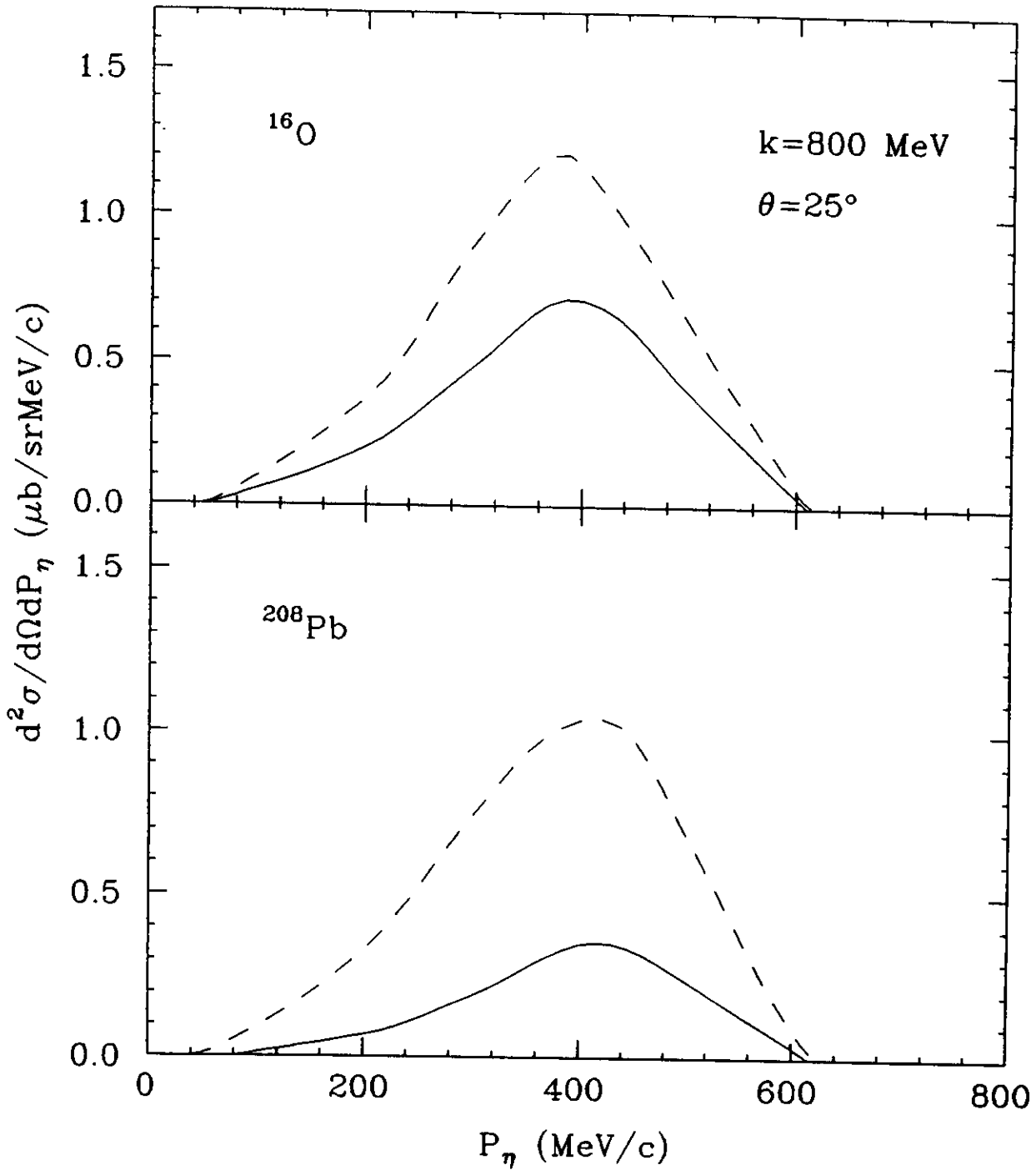

Fig. 3. Differential cross sections for the photoproduction of η mesons in ^{16}O and ^{208}Pb at a photon energy k = 800 MeV and a laboratory angle $\theta = 25^{\circ}$. The solid and dashed curves are the results of calculations with and without final-state interactions, respectively. Figure reproduced form Ref. [18].

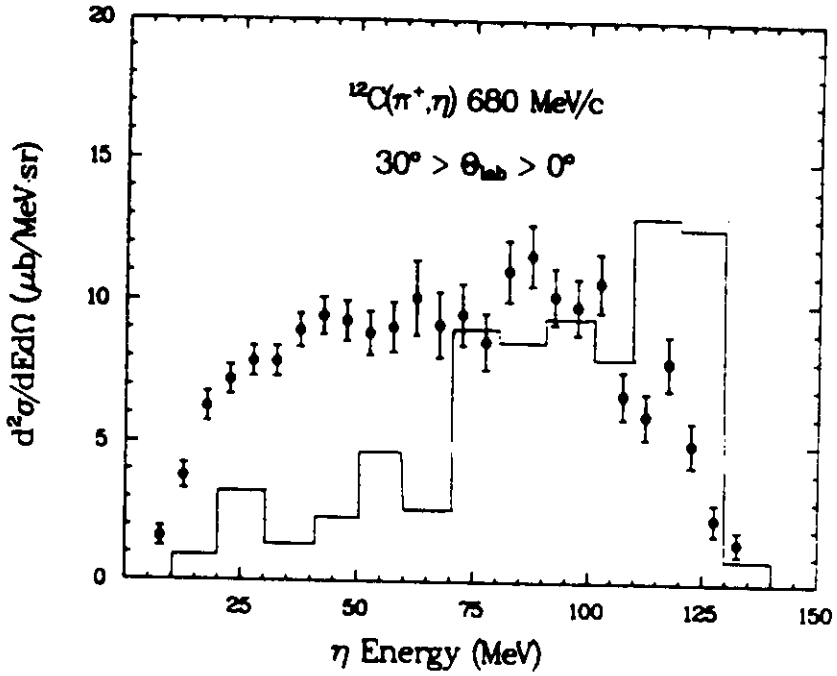

Fig. 4. Inclusive (π^+,η) energy spectrum on ^{12}C at a beam momentum of 680 MeV/c taken from Ref. [20]. The solid curve is a preliminary attempt to reproduce the spectrum.

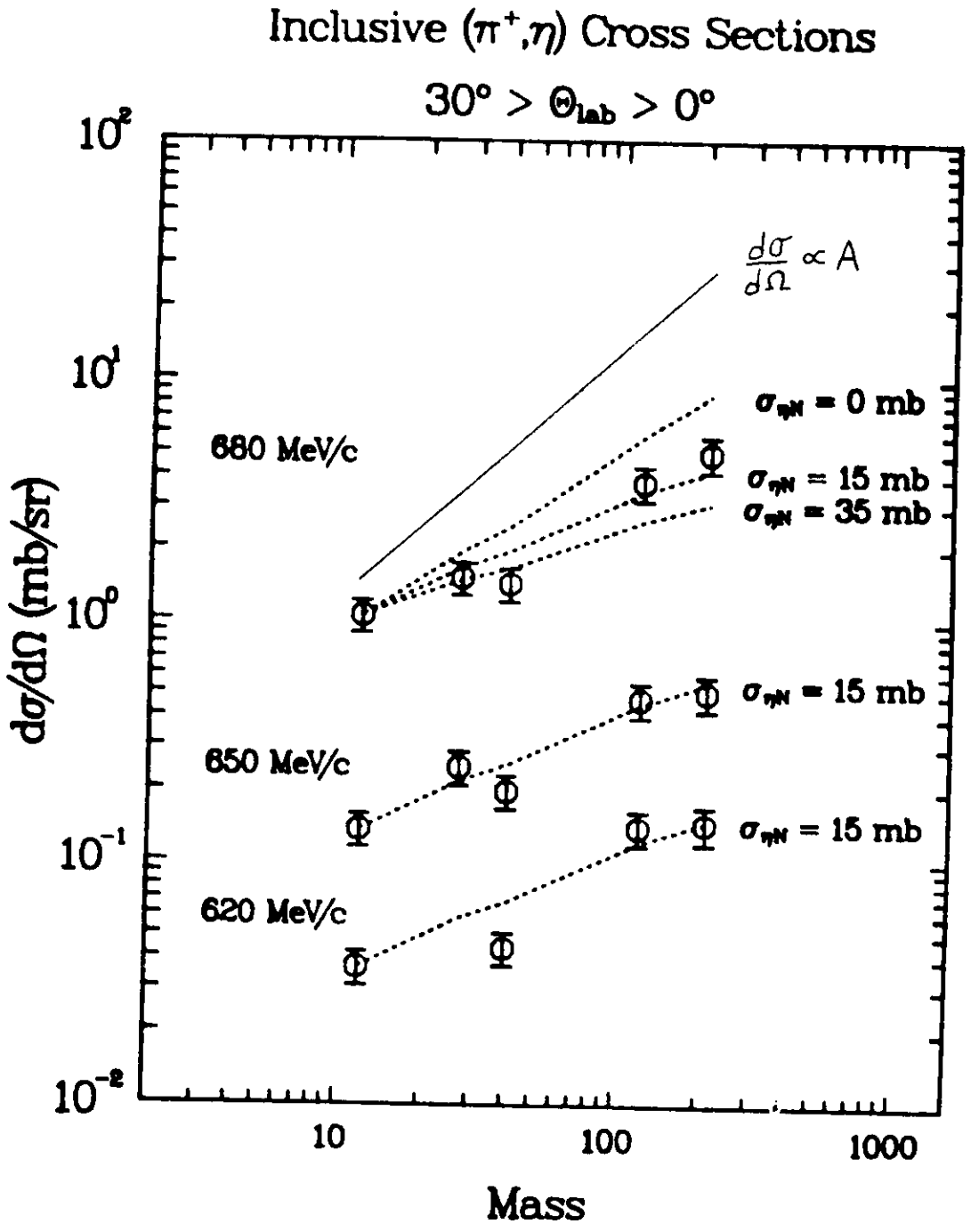

Fig. 5. Target mass dependence of inclusive (π^+,η) cross sections taken from Ref. [20]. The dashed curves are the results of Glauber calculations [25] using various ηN total cross sections. We have added the solid curve to the figure to represent the cross section without final-state or initial-state interactions.

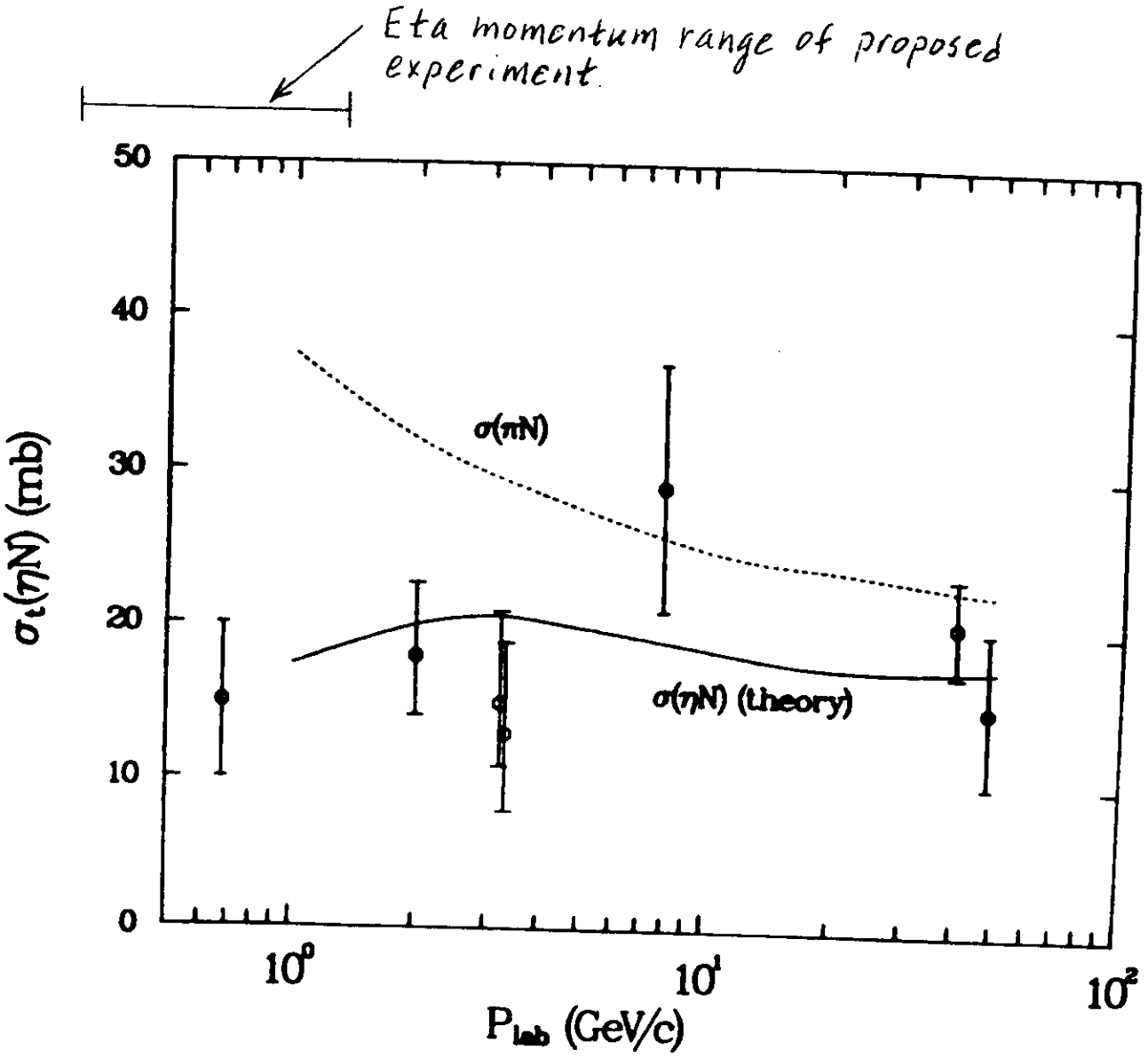

Fig. 6. Eta-nucleon total cross sections as a function of the pion beam momentum taken from Ref. [20]. The solid curve is the prediction of the additive quark model [26] for the ηN total cross sections. The πN total cross section is shown as the dashed curve for comparison. The η momentum range of the proposed experiment is indicated above the figure.

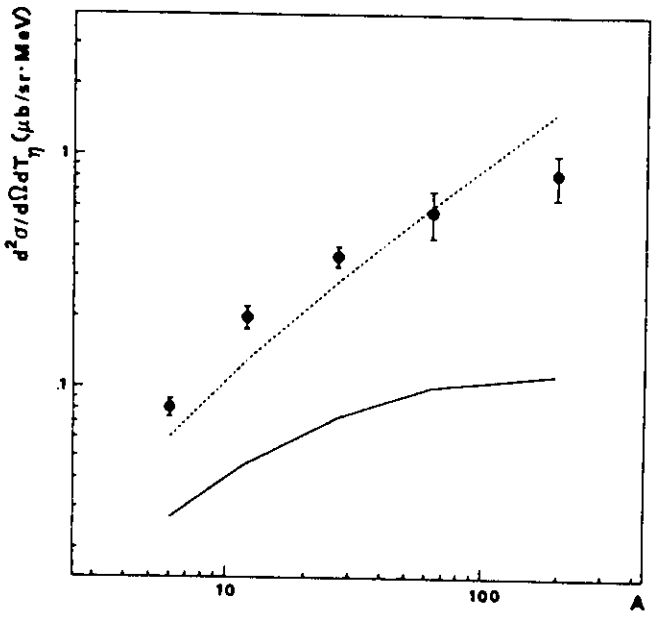

Fig. 7. Differential cross sections for the inclusive A(p,η) reaction at a proton energy of 1 GeV as a function of target mass number A, taken from Ref. [27]. The solid and dashed curves are predictions of the folding model [28] with and without η absorption, respectively.

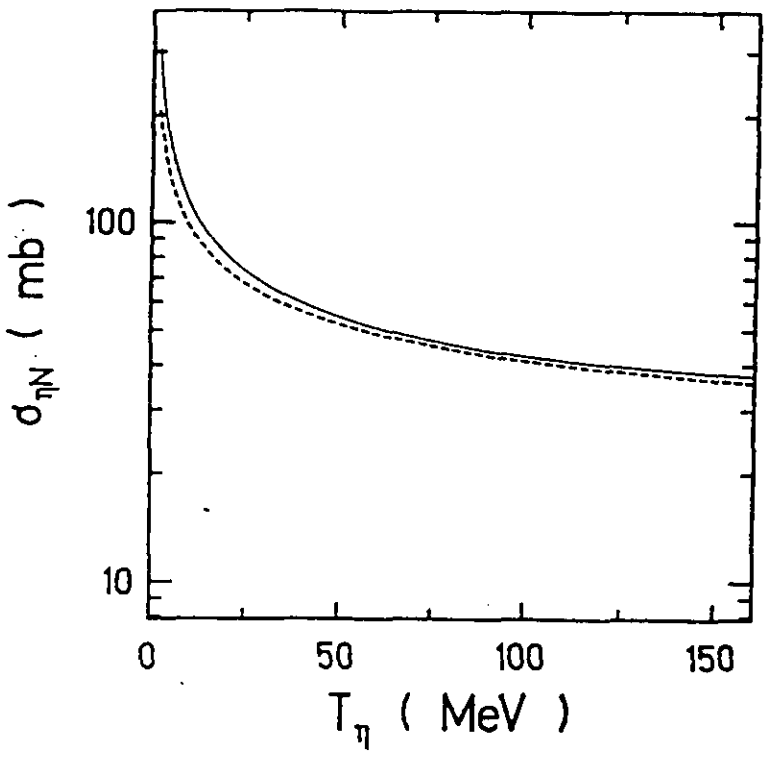

Fig. 8. The total cross section $\sigma_{\eta N}$ (solid curve) as a function of the kinetic energy of the η meson in the nucleon rest frame. The dashed curve is the result of a coupled-channel analysis of Bhalerao and Liu [15]. The figure is taken from Ref. [28].

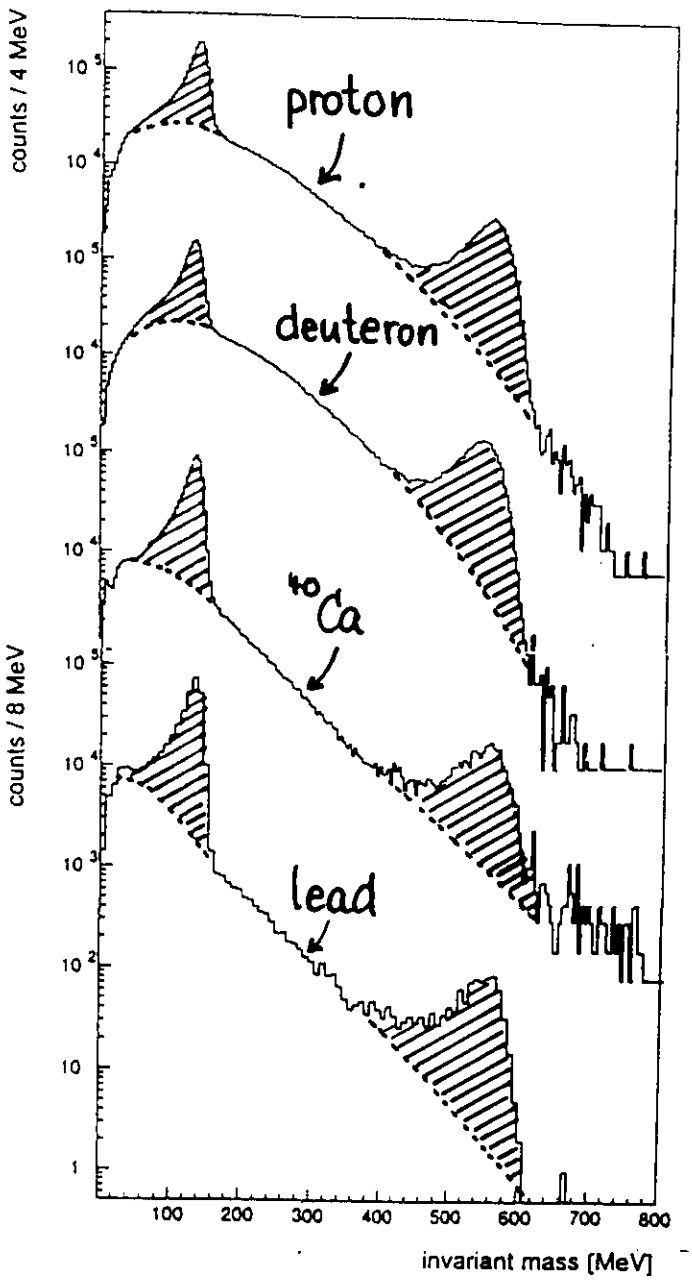

Fig. 9. Invariant mass spectra for photoproduction on ^{1}H, ^{2}H, ^{40}Ca, and ^{nat}Pb targets with incident photons in the energy range 600-790 MeV taken from Ref. [29].

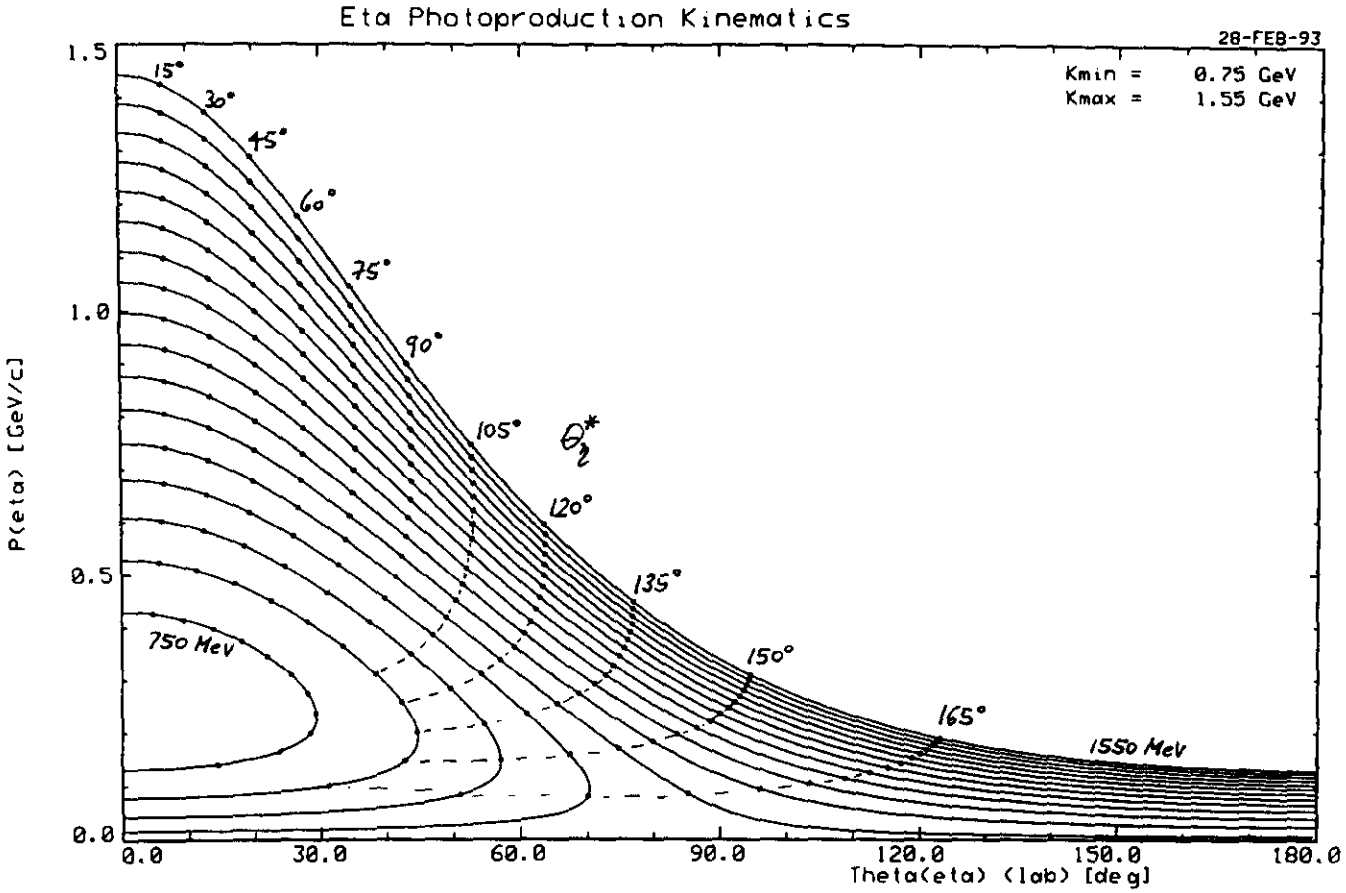

Fig. 10. Eta photoproduction kinematics for incident photon energies between 0.75 and 1.55 GeV.

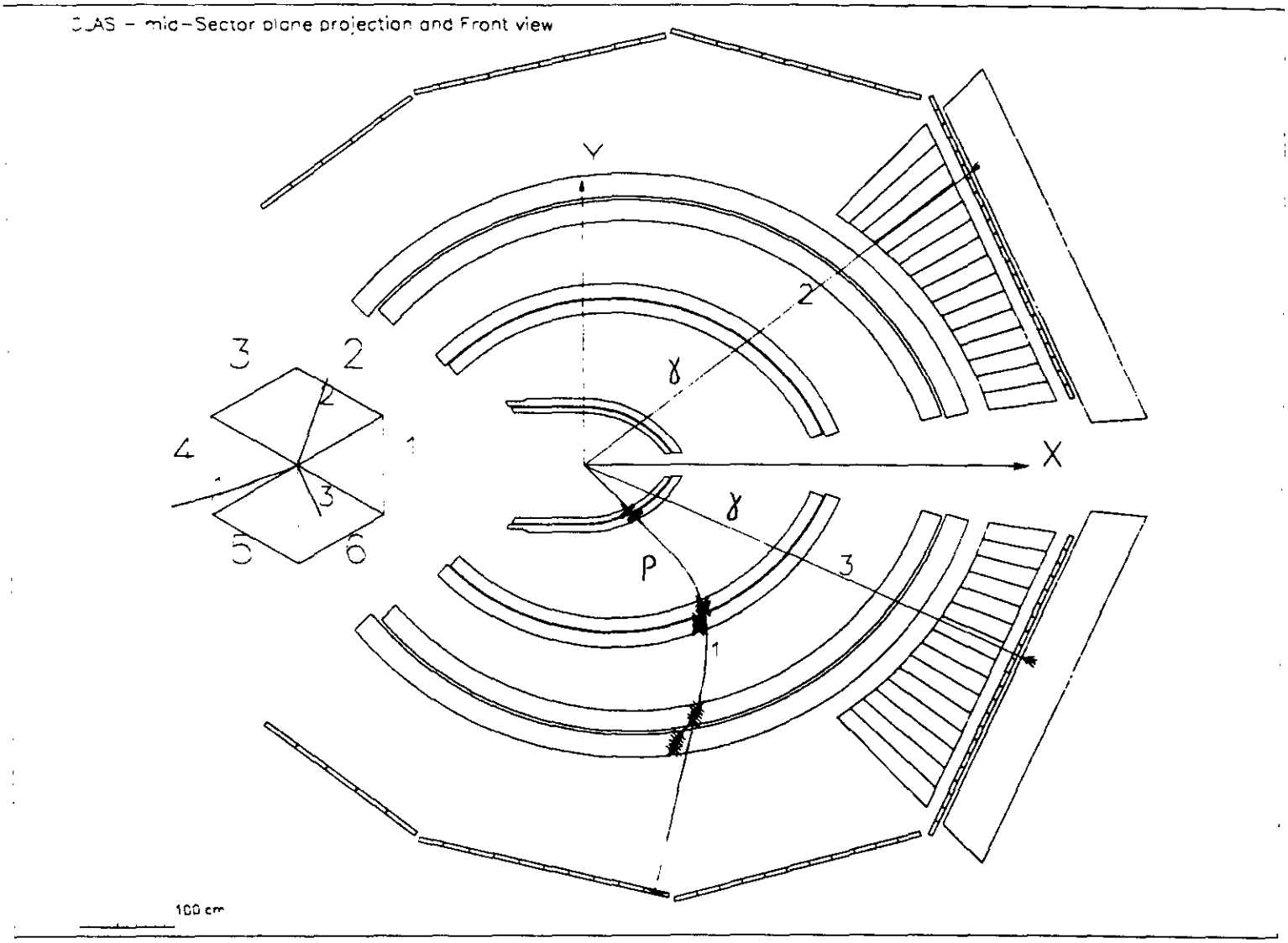

Fig. 11. A typical η photoproduction event in the CLAS. Track 1 is a proton, and tracks 2 and 3 are photons from the 2γ decay of the η meson. The incident photon energy is 1.2 GeV.

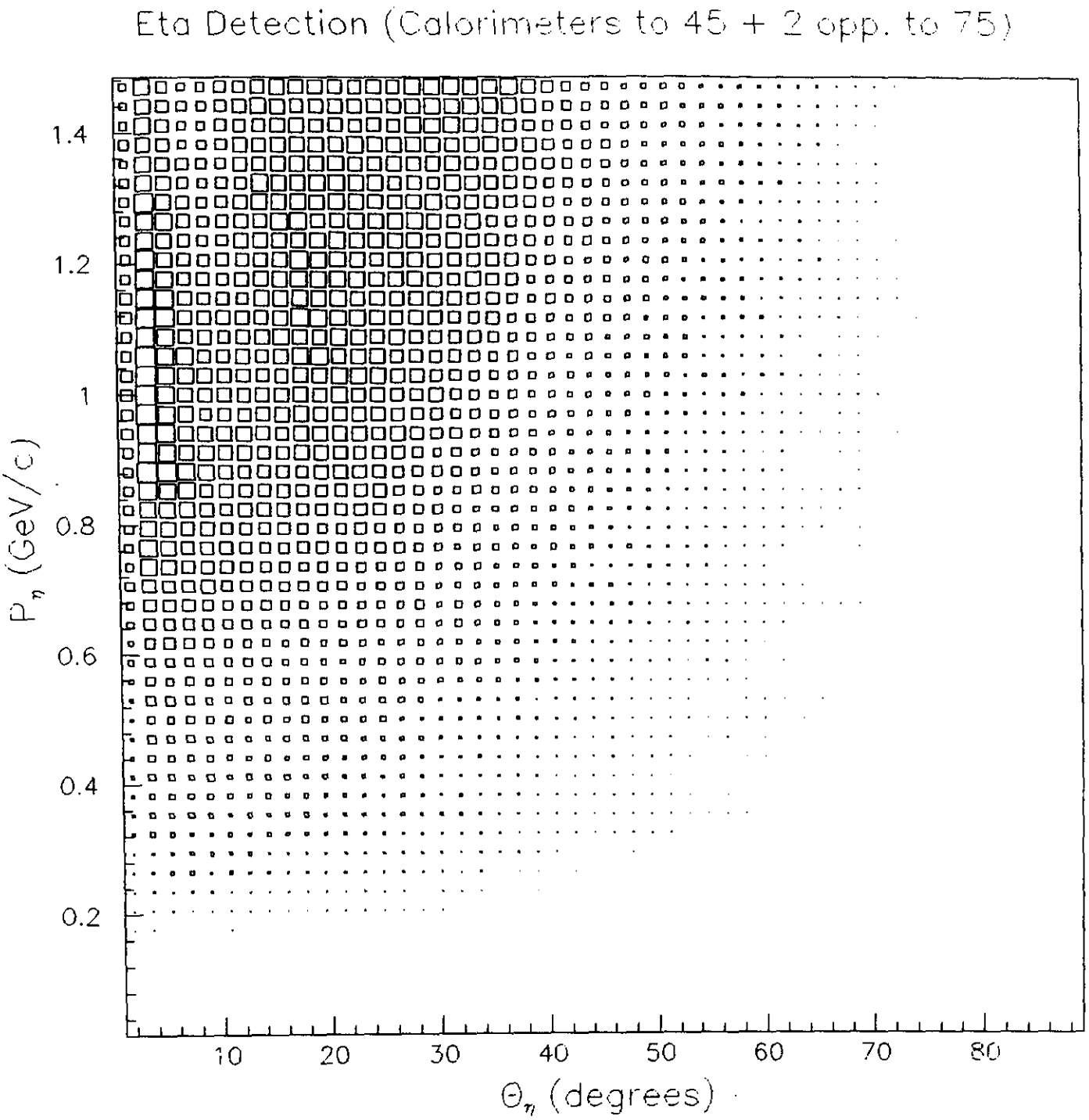

Fig. 12. Eta momentum versus laboratory angle for events accepted by CLAS from a uniform distribution in a Monte Carlo simulation assuming calorimeter coverage from 8° to 45° in six sectors with two additional 30° modules extending the coverage to 75° in two opposite sectors.

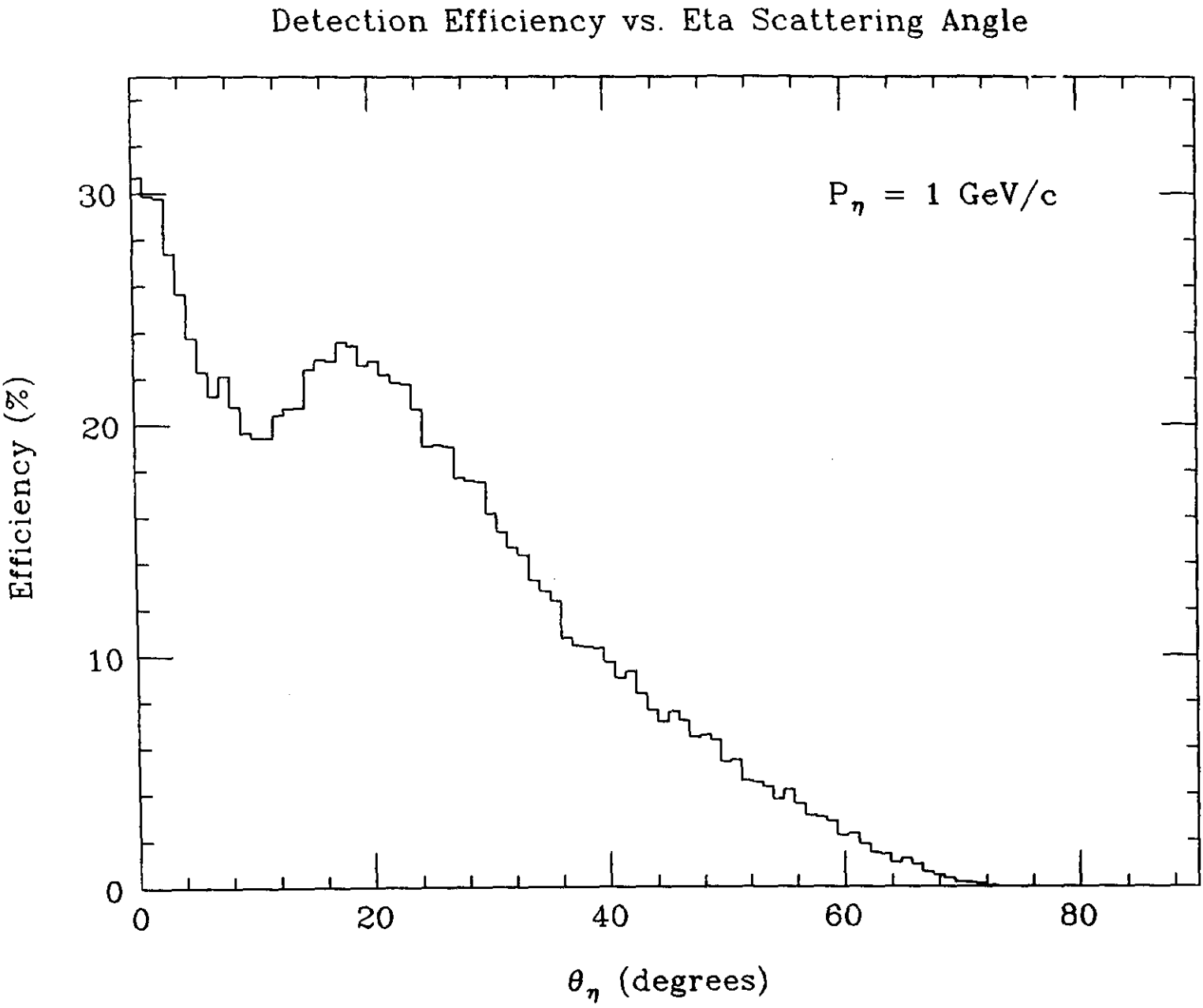

Fig. 13. Detection efficiency as a function of η laboratory angle at P_η = 1.0 GeV/c assuming calorimeter coverage from 8° to 45° in six sectors with two additional 30° modules extending the coverage to 75° in two opposite sectors.

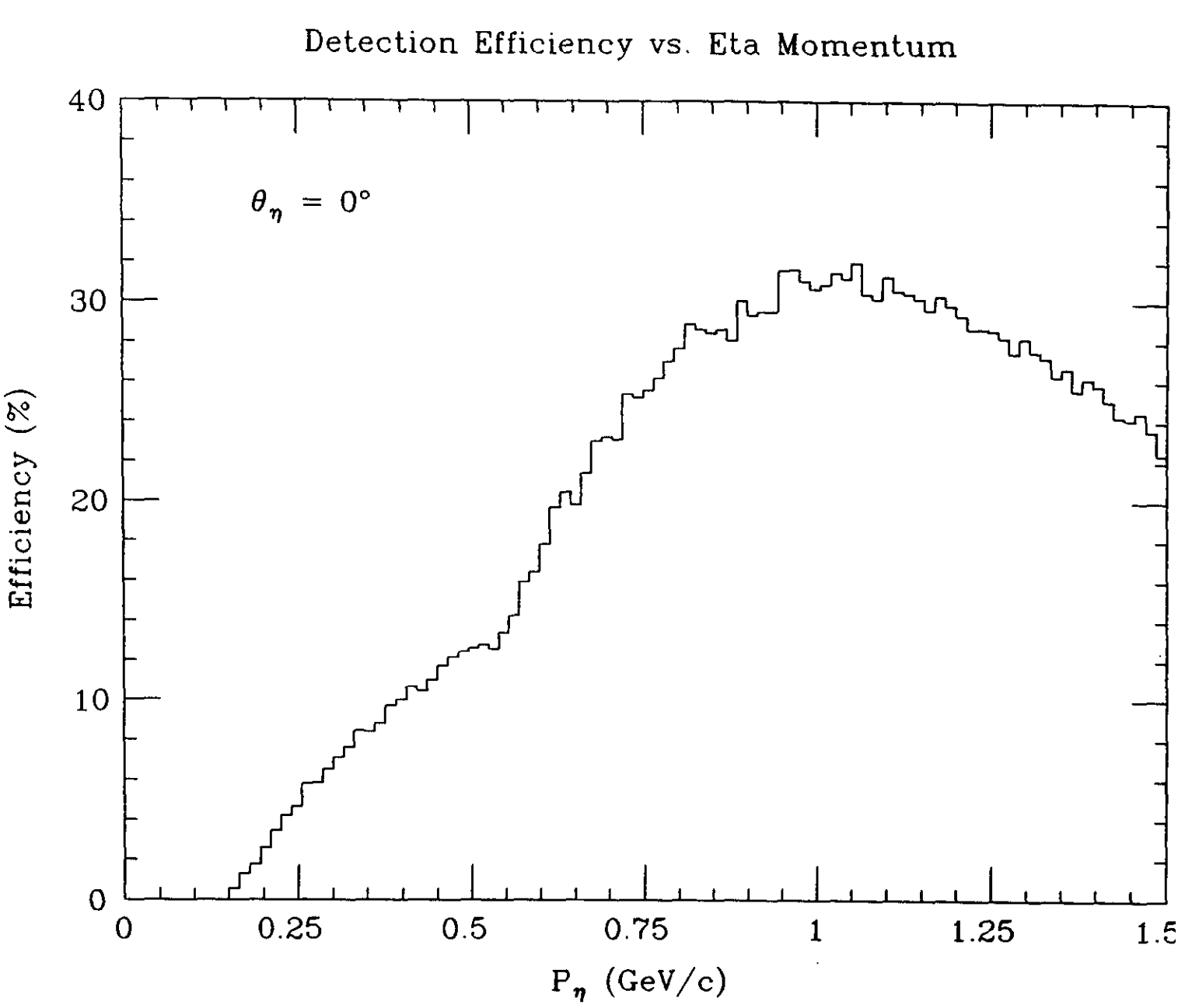

Fig. 14. Detection efficiency as a function of η momentum at $\theta_\eta = 0°$ assuming calorimeter coverage from 8° to 45° in six sectors with two additional 30° modules extending the coverage to 75° in two opposite sectors.

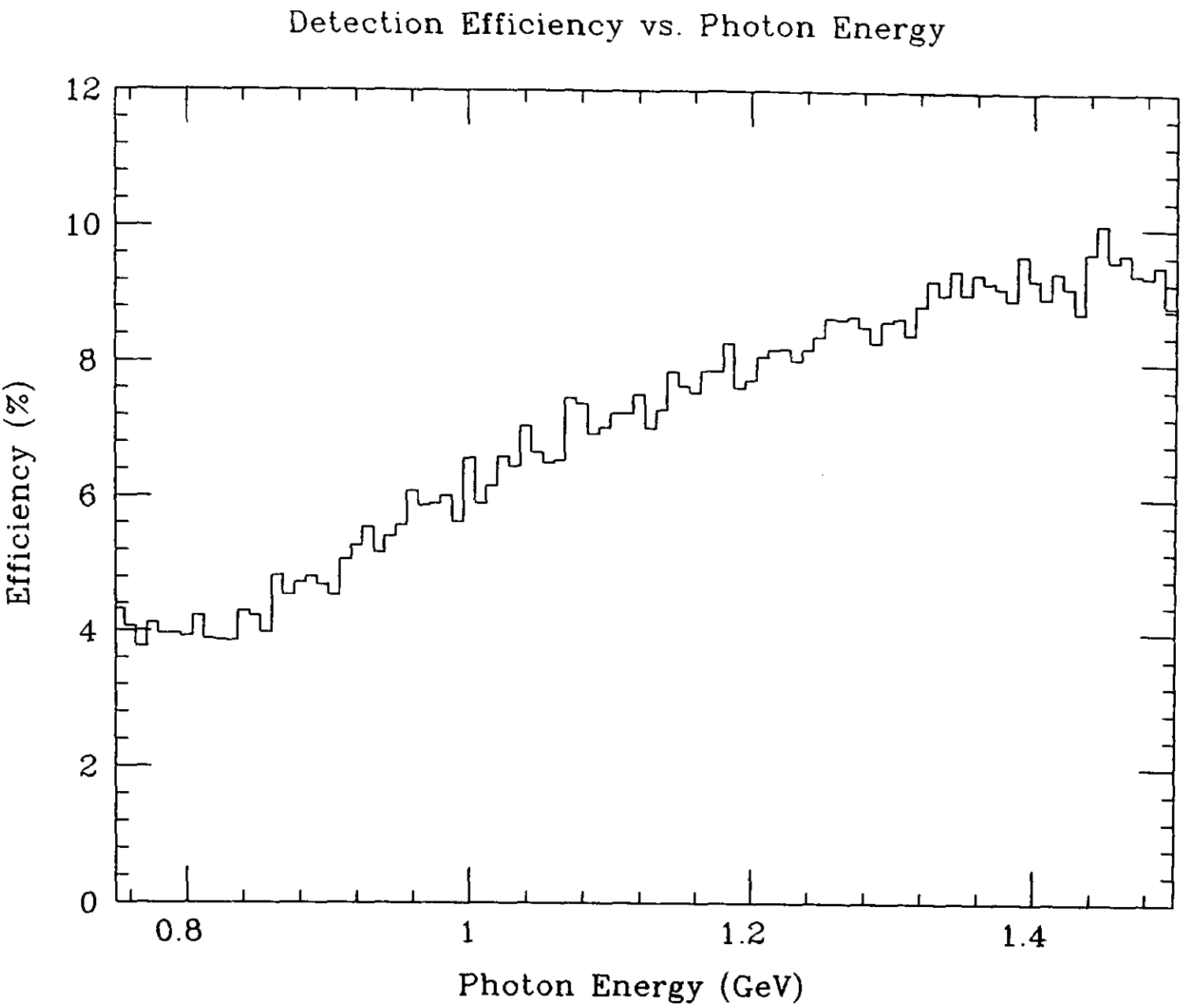

Fig. 15. Detection efficiency as a function of incident photon energy for production on the free proton assuming calorimeter coverage from 8° to 45° in six sectors with two additional 30° modules extending the coverage to 75° in two opposite sectors.

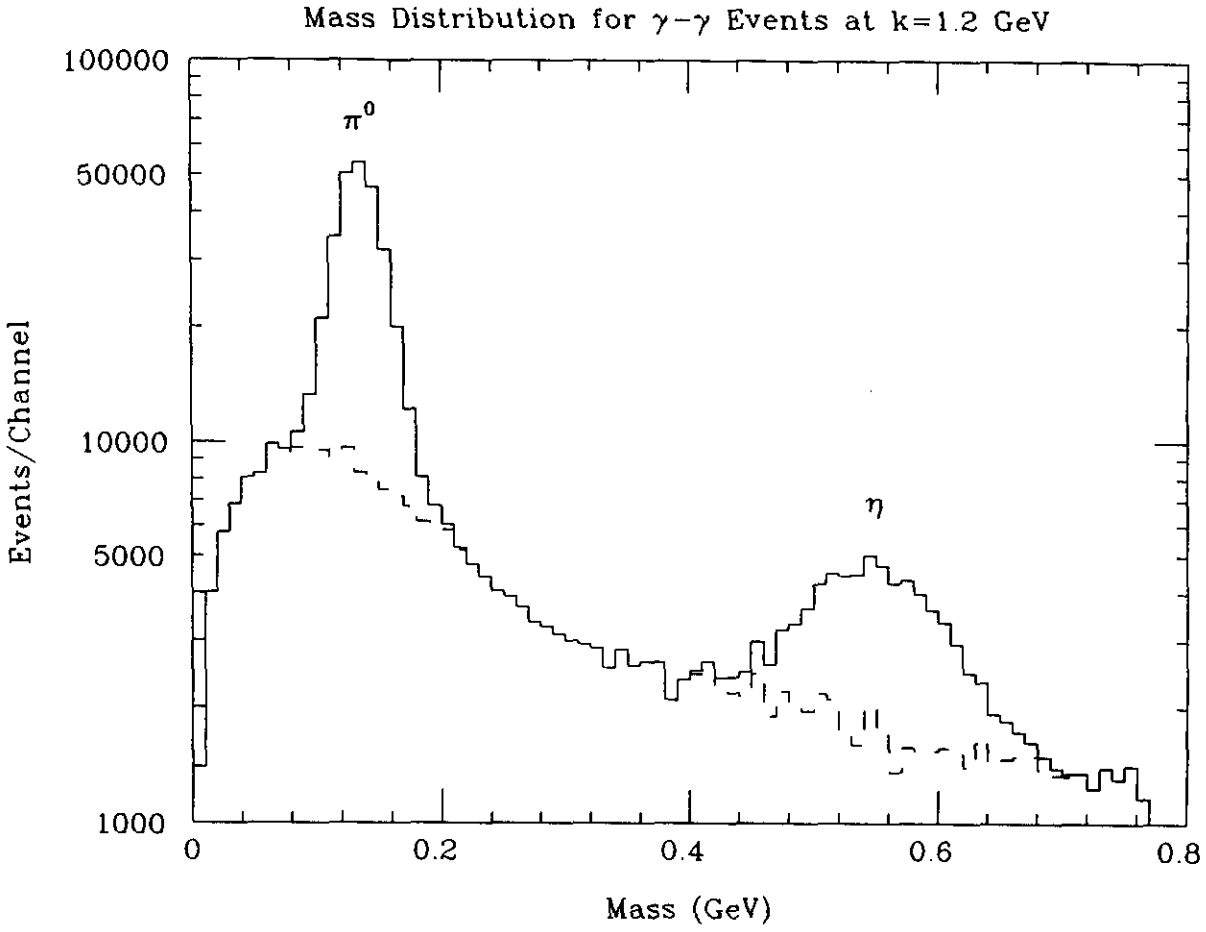

Fig. 16. Simulated mass spectrum for γ-γ events from photoproduction at k = 1.2 GeV. Most of the background (dashed histogram) is from the detection of two coincident photons from different π^0s produced in the $\gamma N \rightarrow \pi^0\pi^0 N$ reaction and the $3\pi^0$ decay of the η meson. The background at large mass is from coincidences between the γ and one of the photons produced in the $\omega \rightarrow \pi^0\gamma$ decay. The background has been suppressed by discriminating against events with more than two photons detected in coincidence.

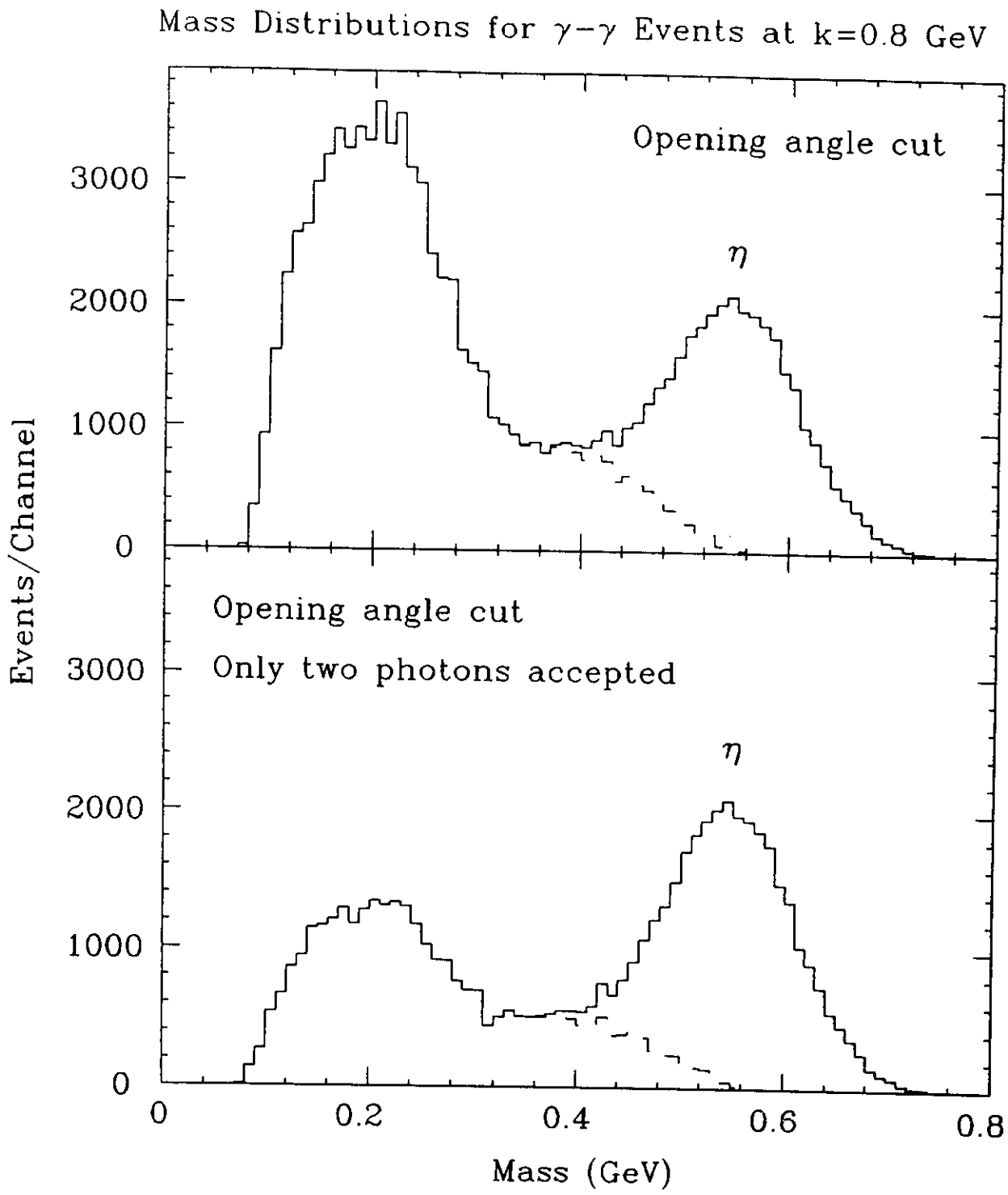

Fig. 17. Simulated mass distributions for γ-γ events from photoproduction at k = 0.8 GeV. The upper distribution was generated with a simple cut on the opening angle to suppress the background. The lower distribution was produced with the additional condition that only two photons are detected.

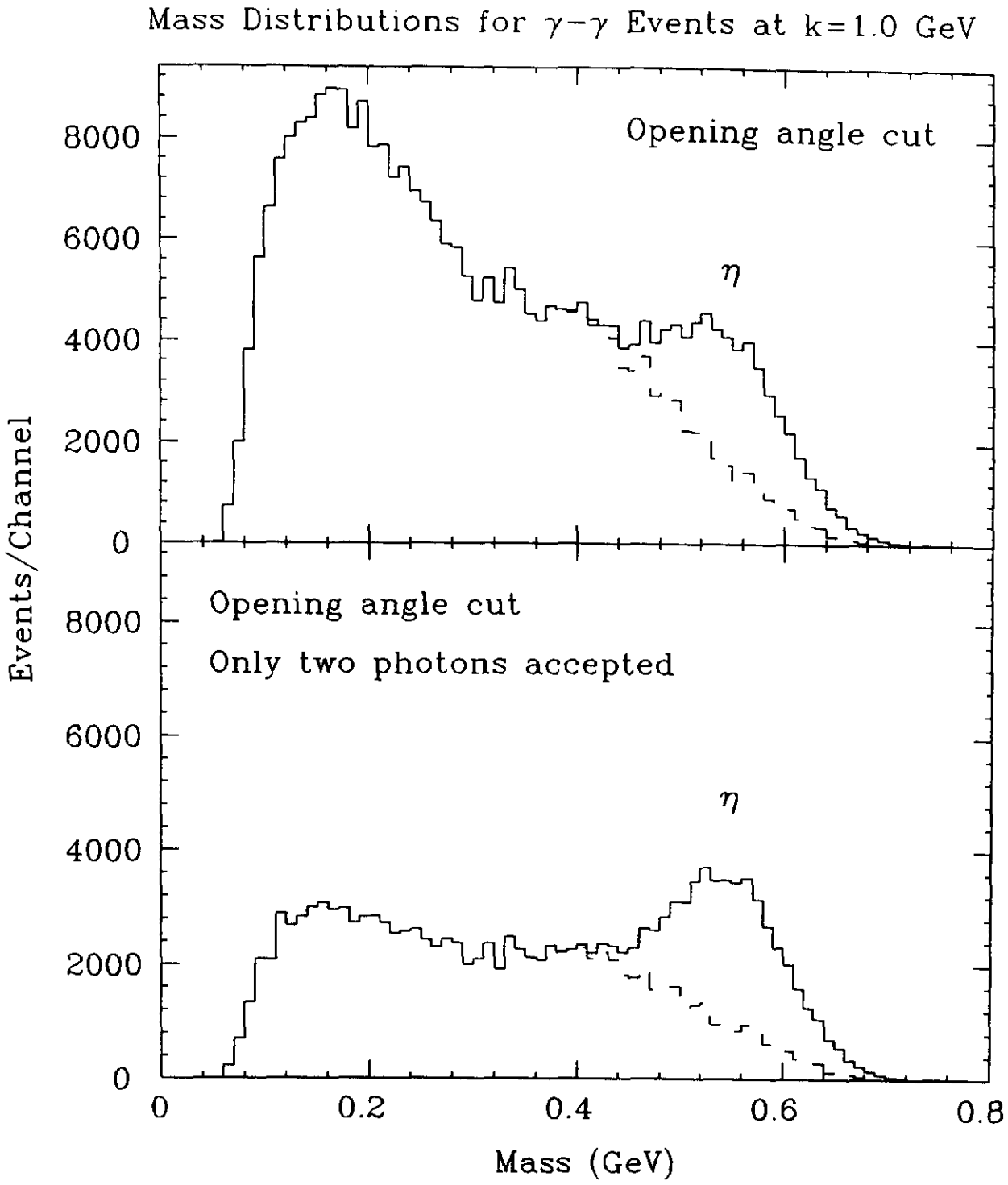

Fig. 18. Same as Fig. 17 except at k = 1.0 GeV.

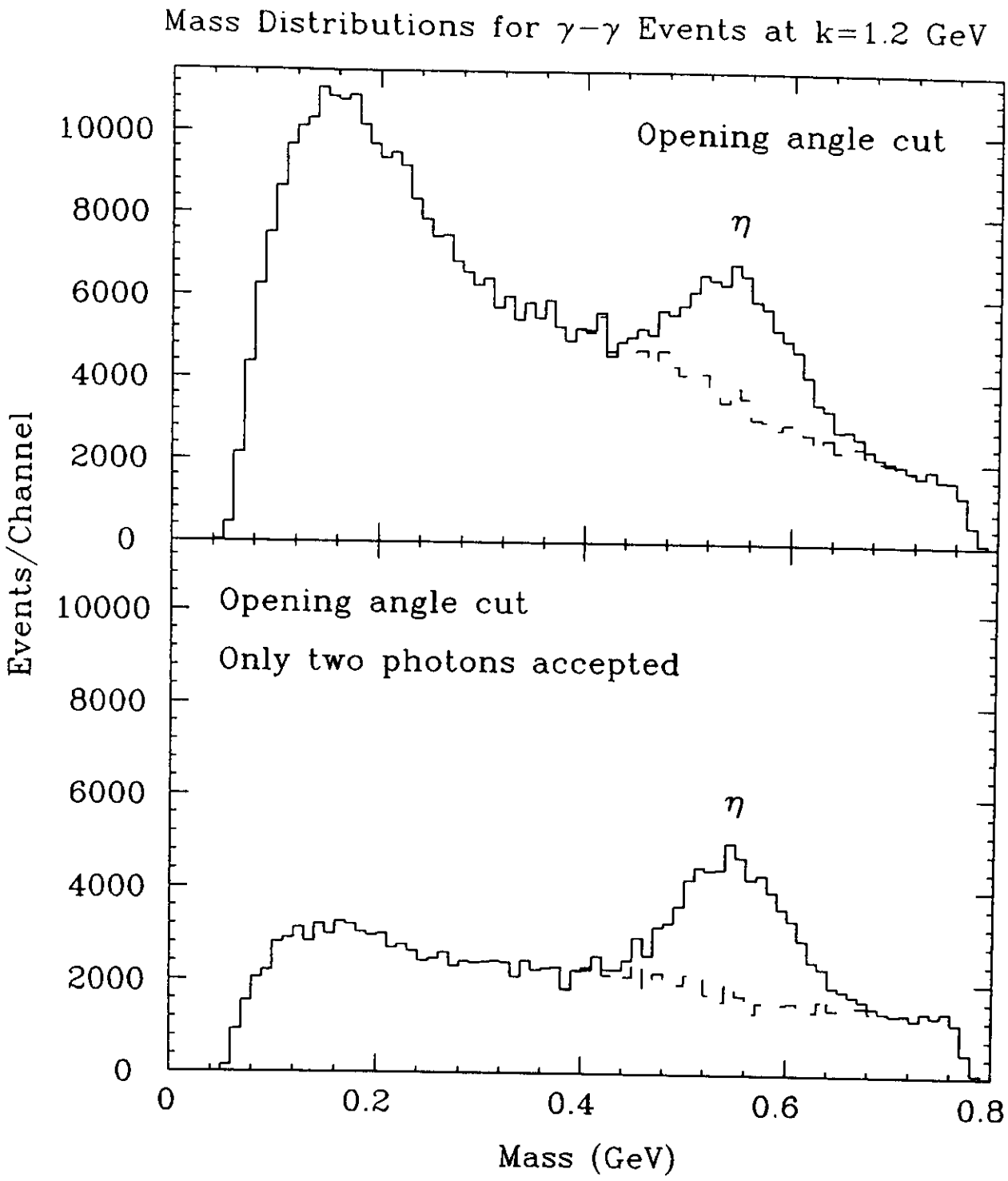

Fig. 19. Same as Fig. 17 except at k = 1.2 GeV.

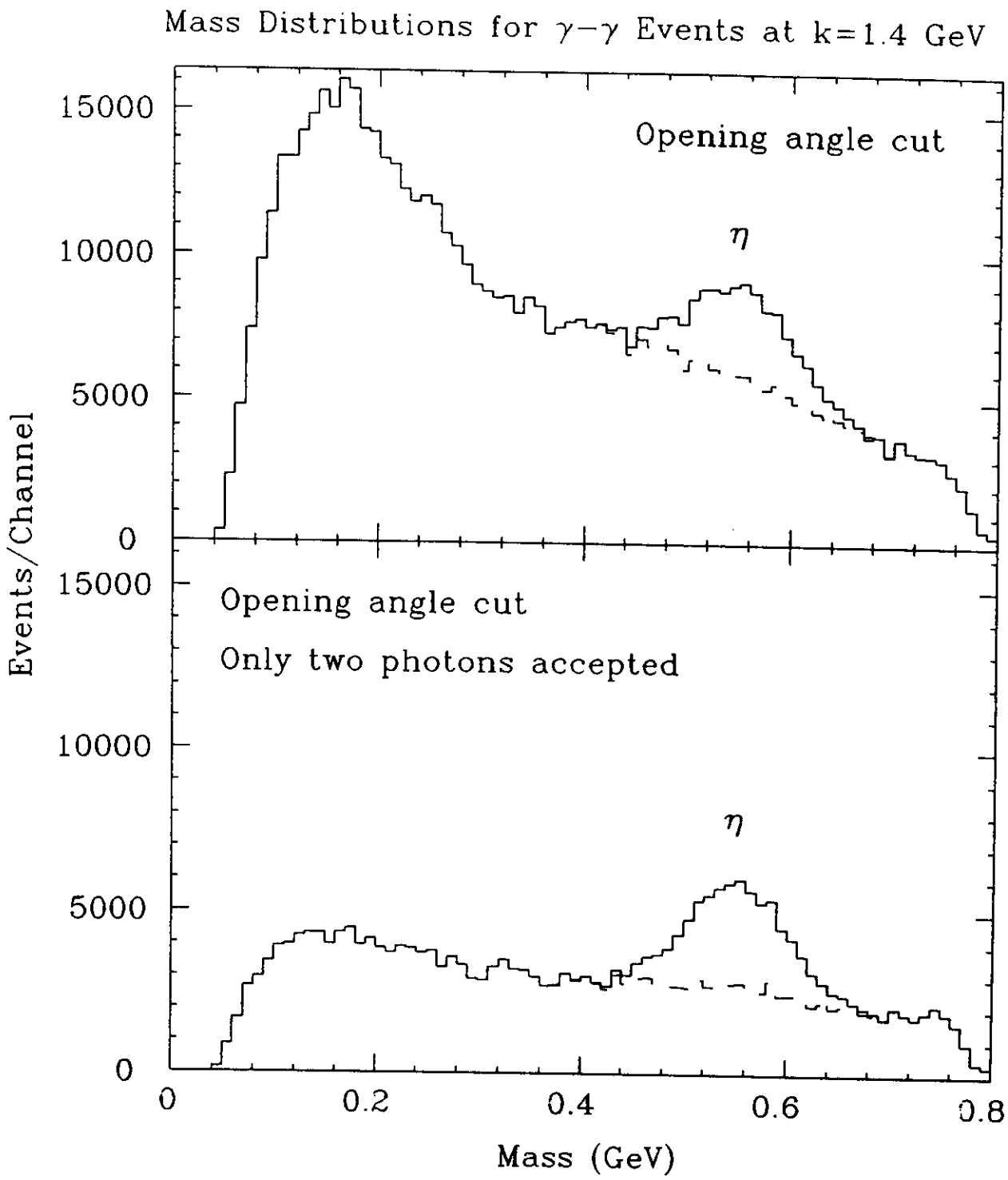

Fig. 20. Same as Fig. 17 except at k = 1.4 GeV.

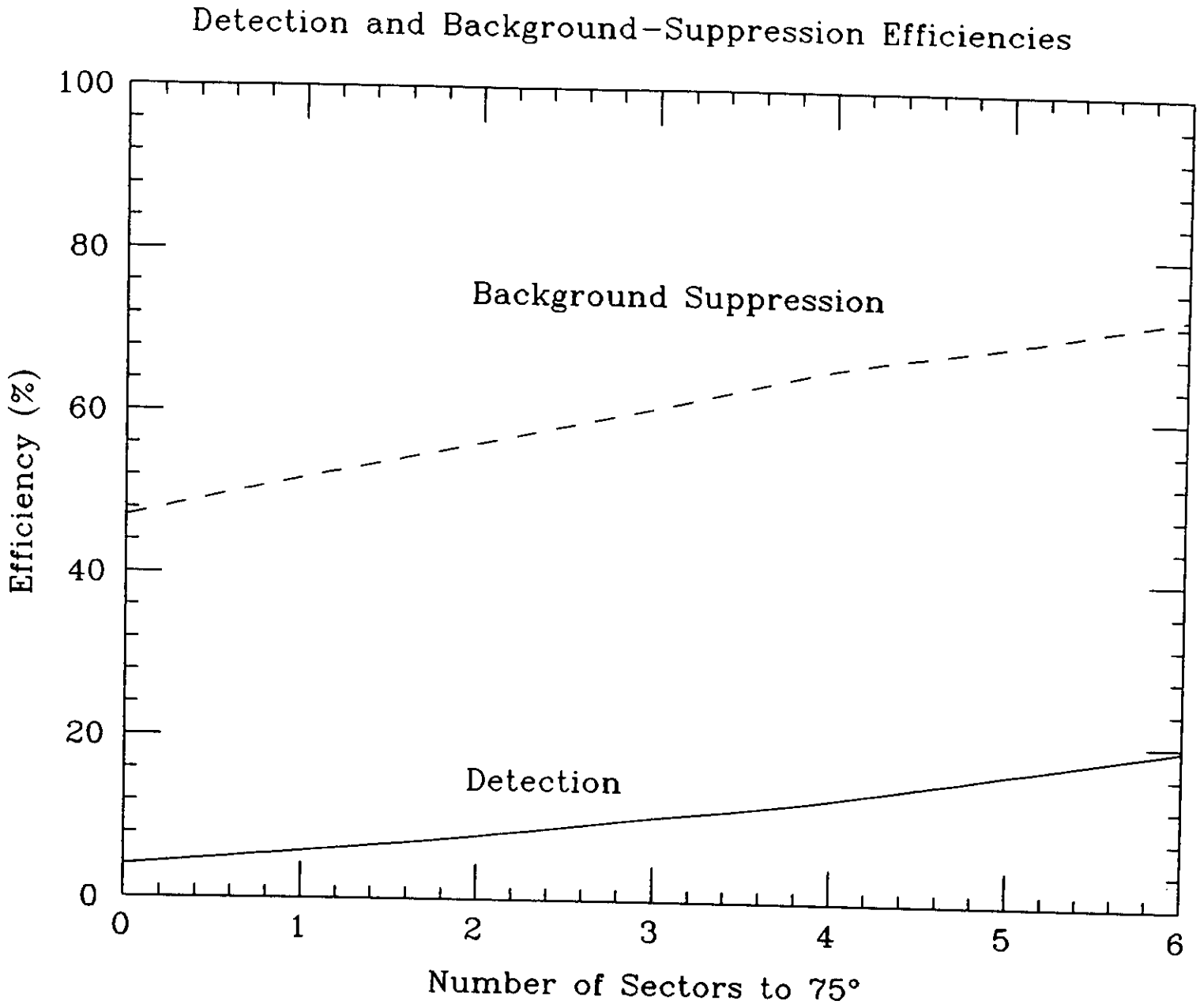

Fig. 21. Detection and background-suppression efficiencies as a function of the number of CLAS sectors with calorimeter coverage extended from 45° to 75°. The efficiencies were determined from Monte Carlo calculations for photoproduction on the free proton at k = 1.2 GeV.

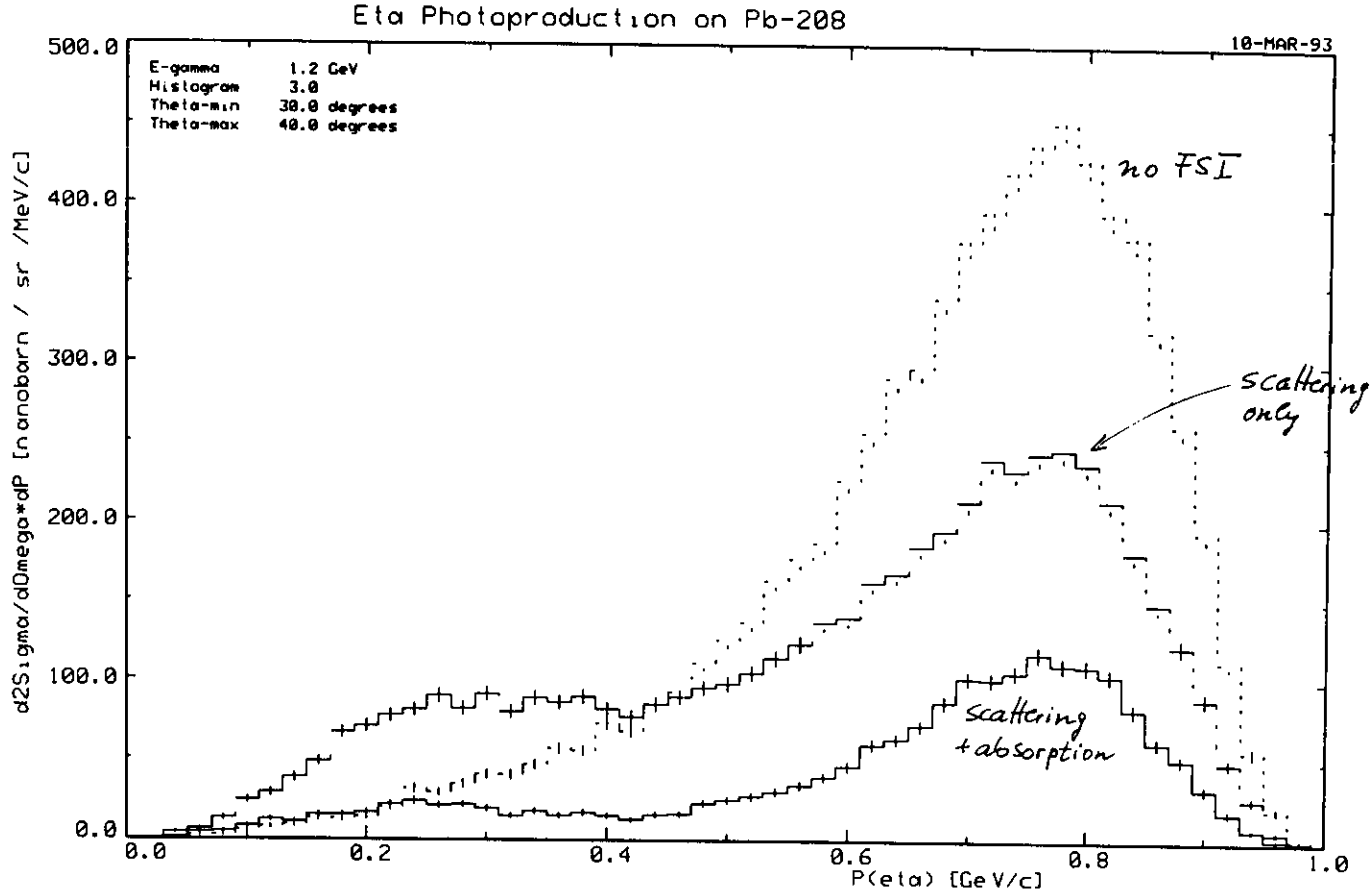

Fig. 22. Momentum distributions for η photoproduction on ^{208}Pb at k = 1.2 GeV and θ_η = 30-40° simulated with intranuclear Monte Carlo calculations. The dotted histogram represents quasifree production with no final-state interactions. The dashed histogram shows the effect of η scattering in the nucleus. The solid histogram is the expected distribution taking into account scattering and absorption.

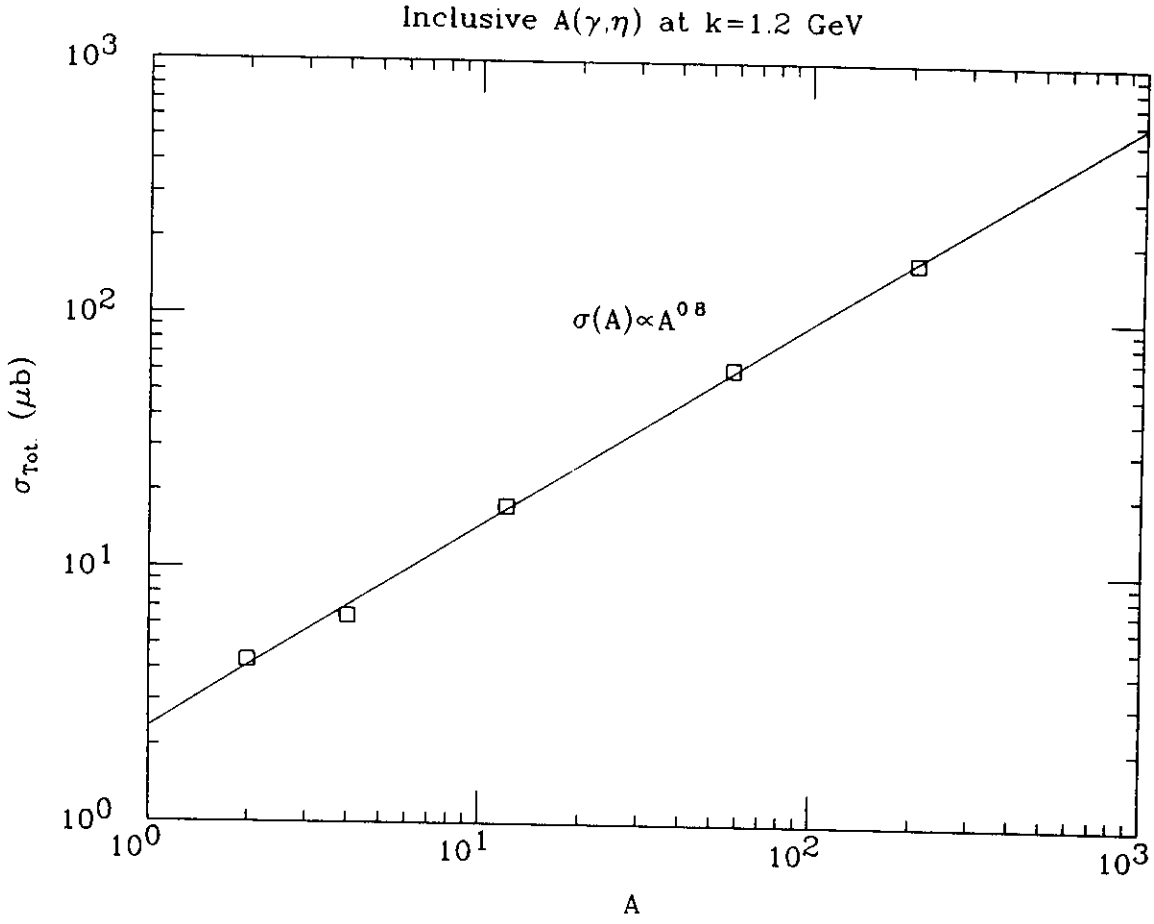

Fig. 23. The A dependence of the total η photoproduction cross sections calculated with an intranuclear Monte Carlo code at k = 1.2 GeV. The cross section scales as $A^{0.8}$.

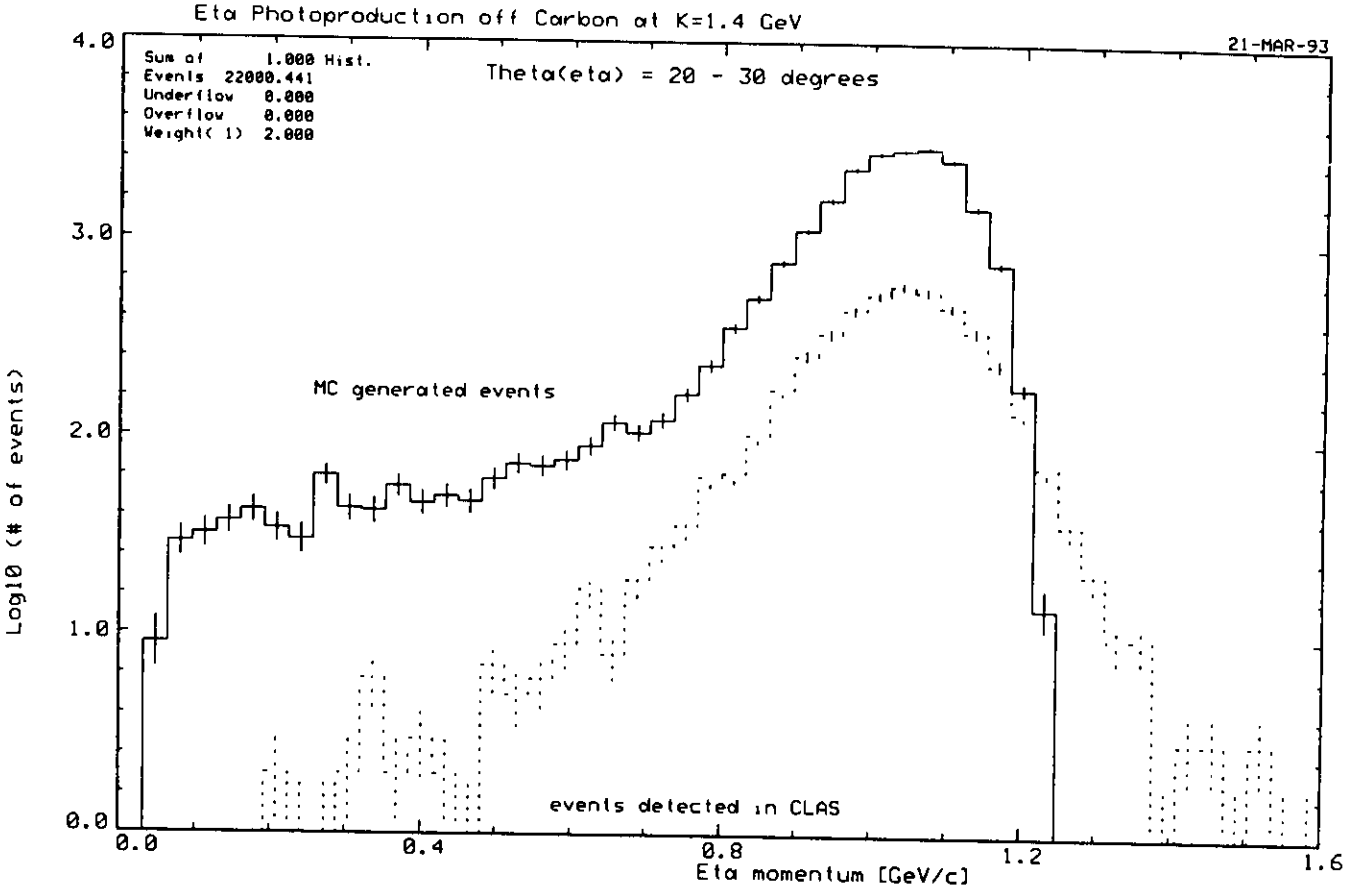

Fig. 24. Simulated momentum distributions expected after 150 hours of running time on ^{12}C at k = 1.4 GeV and θ_η = 20-30°. The solid histogram shows the events generated with an intranuclear Monte Carlo calculation. The dashed histogram represents the events accepted and reconstructed by the CLAS.

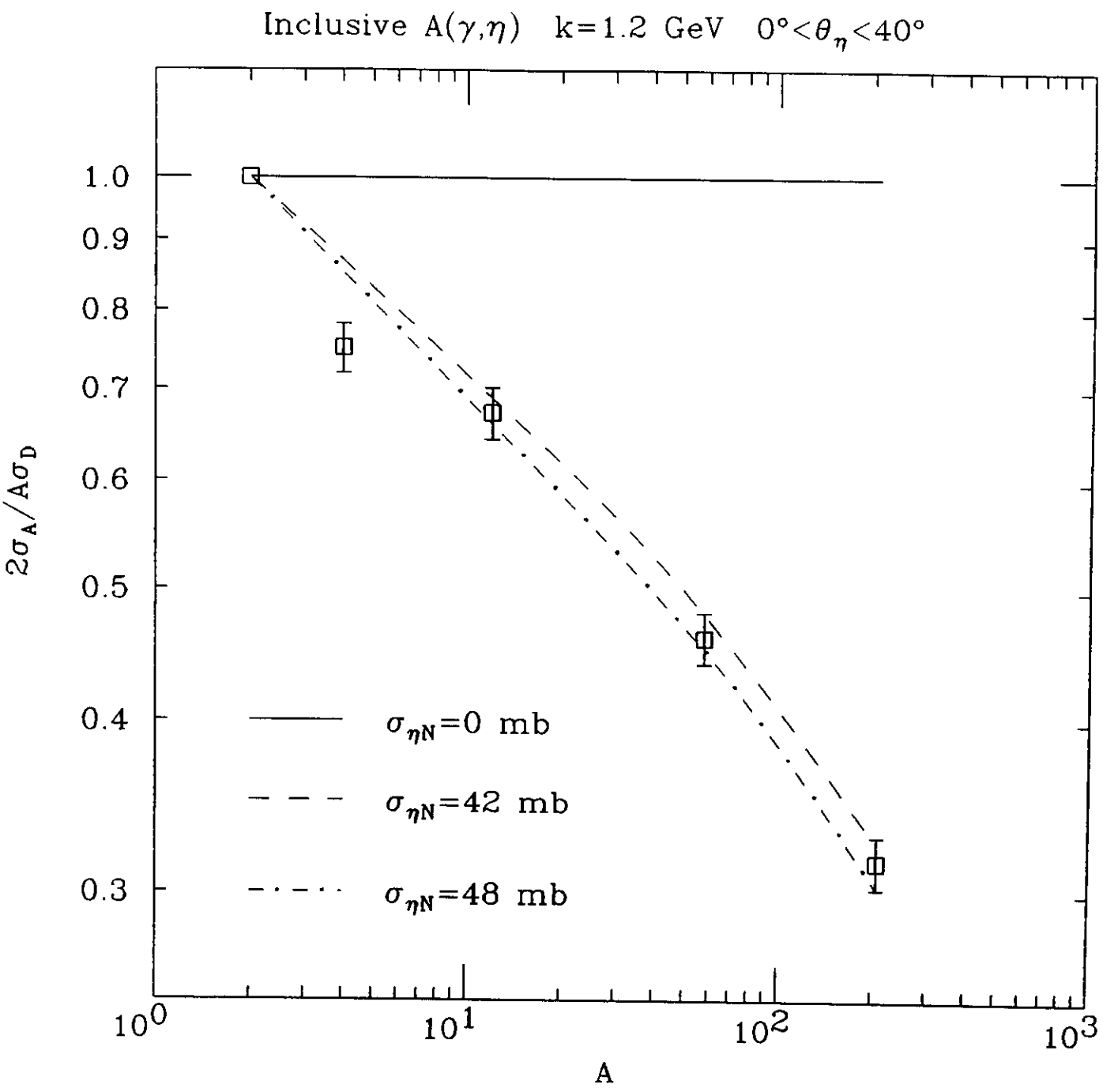

Fig. 25. The A dependence of the ratio of the nuclear cross section per nucleon to the deuteron cross section per nucleon calculated with an intranuclear Monte Carlo cascade code for inclusive η photoproduction at k = 1.2 GeV and $0^\circ < \theta_\eta < 40^\circ$. The solid, dashed, and dot-dashed curves show the results obtained with total ηN cross sections of 0, 42, and 48 mb, respectively.